doi:10.1038/nature10688

FBXO11 targets BCL6 for degradation and is inactivated in diffuse large B-cell lymphomas

Shanshan Duan[1,2]*, Lukas Cermak[1,2]*, Julia K. Pagan[1,2], Mario Rossi[1], Cinzia Martinengo[3], Paola Francia di Celle[4], Bjoern Chapuy[5], Margaret Shipp[5], Roberto Chiarle[3] & Michele Pagano[1,2]

BCL6 is the product of a proto-oncogene implicated in the pathogenesis of human B-cell lymphomas[1,2]. By binding specific DNA sequences, BCL6 controls the transcription of a variety of genes involved in B-cell development, differentiation and activation. BCL6 is overexpressed in the majority of patients with aggressive diffuse large B-cell lymphoma (DLBCL), the most common lymphoma in adulthood, and transgenic mice constitutively expressing BCL6 in B cells develop DLBCLs similar to the human disease[3,4]. In many DLBCL patients, BCL6 overexpression is achieved through translocation (~40%) or hypermutation of its promoter (~15%). However, many other DLBCLs overexpress BCL6 through an unknown mechanism. Here we show that BCL6 is targeted for ubiquitylation and proteasomal degradation by a SKP1–CUL1–F-box protein (SCF) ubiquitin ligase complex that contains the orphan F-box protein FBXO11 (refs 5, 6). The gene encoding FBXO11 was found to be deleted or mutated in multiple DLBCL cell lines, and this inactivation of *FBXO11* correlated with increased levels and stability of BCL6. Similarly, *FBXO11* was either deleted or mutated in primary DLBCLs. Notably, tumour-derived FBXO11 mutants displayed an impaired ability to induce BCL6 degradation. Reconstitution of FBXO11 expression in *FBXO11*-deleted DLBCL cells promoted BCL6 ubiquitylation and degradation, inhibited cell proliferation, and induced cell death. *FBXO11*-deleted DLBCL cells generated tumours in immunodeficient mice, and the tumorigenicity was suppressed by FBXO11 reconstitution. We reveal a molecular mechanism controlling BCL6 stability and propose that mutations and deletions in *FBXO11* contribute to lymphomagenesis through BCL6 stabilization. The deletions/mutations found in DLBCLs are largely monoallelic, indicating that *FBXO11* is a haplo-insufficient tumour suppressor gene.

Because the degradation of BCL6 has been reported to be phosphorylation-dependent[7,8], we examined the hypothesis that BCL6 is degraded by an SCF ubiquitin ligase complex, as most SCF ligases target phosphorylated substrates[5]. The expression of a dominant-negative CUL1 mutant (CUL1(1–242) or CUL1(1–385)) results in the accumulation of SCF substrates[9–11]. Western blotting of extracts from Ramos cells (a Burkitt's lymphoma cell line) infected with a retrovirus expressing CUL1(1–385) revealed that BCL6 level was increased compared to control cells, indicating that BCL6 is an SCF substrate (Supplementary Fig. 1a). Similarly, silencing RBX1, another SCF subunit, induced the accumulation of BCL6 (Supplementary Fig. 1b). Therefore, we investigated the ability of BCL6 to be recruited to the SCF via a panel of F-box proteins. Screening of a library of F-box proteins (ten shown) revealed that BCL6 specifically bound FBXO11 (Fig. 1a and Supplementary Fig. 2a), and this binding was confirmed with endogenous proteins in both Ramos cells (Fig. 1b) and primary B cells from mice (Supplementary Fig. 2b). Moreover, BCL6 was found to interact with endogenous SKP1 and neddylated CUL1, the form of CUL1 that

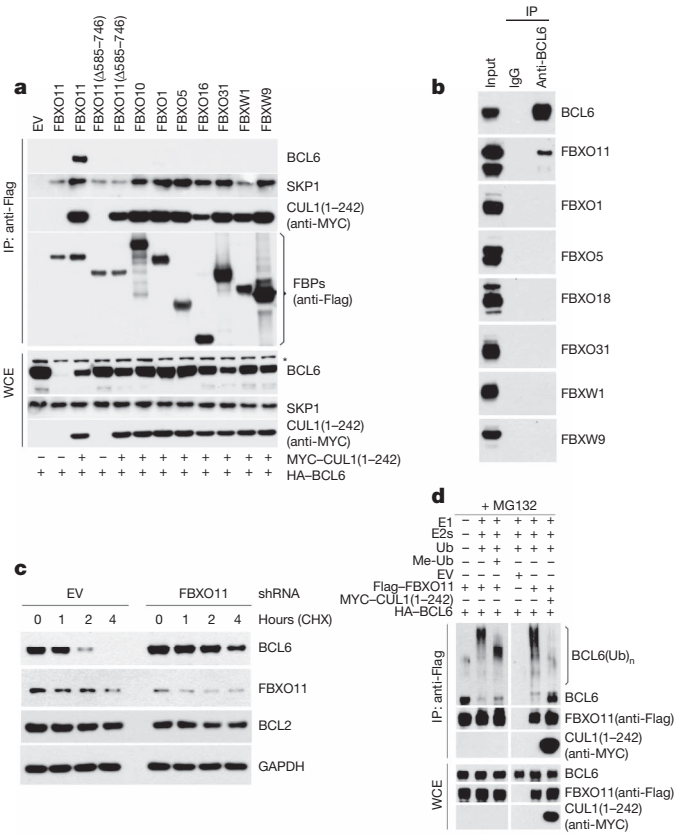

Figure 1 | FBXO11 controls the ubiquitylation and degradation of BCL6. **a**, HEK-293T cells were transfected with HA-tagged BCL6 and the indicated Flag-tagged F-box proteins (FBPs) or an empty vector (EV). Where indicated, MYC-tagged CUL1(1–242) was also transfected. Twenty-four hours after transfection, cells were harvested and lysed. Whole-cell extracts (WCE) were subjected to immunoprecipitation (IP) with anti-Flag resin and immunoblotting as indicated. The asterisk denotes a nonspecific band present in the anti-BCL6 blot. **b**, Ramos cells were treated with MG132 during the last 5 h before lysis. Lysates were immunoprecipitated with either an antibody against BCL6 or a nonspecific IgG and analysed by immunoblotting as indicated. **c**, SU-DHL6 cells were infected with viruses expressing two different *FBXO11* shRNAs (in combination) or a control shRNA, selected, and treated with cycloheximide for the indicated times. Protein extracts were immunoblotted for the indicated proteins. **d**, HEK-293T cells were transfected with HA-tagged BCL6, Flag-tagged FBXO11, MYC-tagged CUL1(1–242), and/or an empty vector (EV) as indicated. After immunopurification with anti-Flag resin, *in vitro* ubiquitylation of BCL6 was performed in the presence or absence of E1, E2s and ubiquitin (Ub). Where indicated, methylated ubiquitin (Me-Ub) was added. Samples were analysed by immunoblotting with an anti-BCL6 antibody. The bracket on the right marks a ladder of bands >86 kDa corresponding to ubiquitylated BCL6. Immunoblots of whole-cell extracts are shown at the bottom.

[1]Department of Pathology, NYU Cancer Institute, New York University School of Medicine, 522 First Avenue, SRB 1107, New York, New York 10016, USA. [2]Howard Hughes Medical Institute, New York University School of Medicine, 522 First Avenue, SRB 1107, New York, New York 10016, USA. [3]Department of Biomedical Sciences and Human Oncology, CERMS, University of Torino, 10126 Torino, Italy. [4]San Giovanni Battista Hospital, Via Santena 7, 10126 Torino, Italy. [5]Medical Oncology, Dana-Farber Cancer Institute, 44 Binney Street, Boston, Massachusetts 02115, USA.
*These authors contributed equally to this work.

preferentially binds SCF substrates[12] (Supplementary Fig. 2a). We also found that BCL6 and FBXO11 co-localized in the nucleus where they showed overlapping, punctate staining throughout the nucleoplasm (Supplementary Fig. 3). Moreover, expression of FBXO11 resulted in a marked reduction of BCL6 levels (Supplementary Fig. 4). This reduction in protein level was due to enhanced proteolysis, as shown by the decrease in BCL6 half-life (Supplementary Fig. 4a, b) and the rescue of BCL6 levels by either CUL1(1–242) (compare lanes 2 and 3 in whole-cell extract of Fig. 1a) or the addition of MG132, a proteasome inhibitor (Supplementary Fig. 3). In contrast, none of the other 20 F-box proteins tested promoted a reduction in BCL6 levels or stability (Supplementary Fig. 4 and data not shown).

To test further whether FBXO11 regulates the degradation of BCL6, we used two short hairpin RNA (shRNA) constructs to reduce FBXO11 expression in Ramos and SU-DHL6 cells. Depletion of FBXO11 by both shRNAs induced an increase in the steady-state levels and stability of BCL6 (Fig. 1c and Supplementary Fig. 5a, b). Similar effects were observed when the cellular expression of FBXO11 was silenced using three additional shRNAs or four different short interfering RNAs (siRNAs; Supplementary Fig. 5c–e).

We also observed that treatment of cells expressing FBXO11 with MG132 induced the appearance of high molecular mass species of BCL6 (Supplementary Fig. 6). These high molecular mass species are strongly induced by the expression of FBXO11 and are probably ubiquitylated forms of BCL6 as they became more evident in the presence of overexpressed ubiquitin. Moreover, we reconstituted the ubiquitylation of BCL6 *in vitro*. Immunopurified FBXO11 promoted the *in vitro* ubiquitylation of BCL6 only when the E1 and E2 enzymes were present in the reaction, and the ubiquitylation was inhibited by the presence of CUL1(1–242) (Fig. 1d). Methylated ubiquitin inhibited the formation of the highest molecular mass forms of BCL6, demonstrating that the high molecular mass forms of BCL6 are indeed polyubiquitylated. These results support the hypothesis that FBXO11 directly controls the ubiquitin-mediated degradation of BCL6.

Notably, FBXO11 silencing induced BCL6 stabilization in the absence of ligand-mediated receptor activation (Fig. 1c and Supplementary Fig. 5), which has been reported to accelerate BCL6 degradation by stimulating its ERK-dependent phosphorylation[7]. Accordingly, the binding of FBXO11 to BCL6 was unaffected in Ramos cells incubated with anti-IgM antibodies (a treatment that mimics B-cell antigen-receptor signalling and activates ERK2 (ref. 7)) both in the presence or absence of PD98059, a MEK inhibitor (Supplementary Fig. 7a). Similarly, when immunopurified BCL6 was phosphorylated *in vitro* by ERK2 or treated with λ-phosphatase, its binding to FBXO11 was unaffected (Supplementary Fig. 7b, c). Finally, a BCL6 mutant lacking the residues phosphorylated by ERK1/2 still bound FBXO11 efficiently (Supplementary Fig. 7d). Together, these results indicate that the FBXO11-dependent degradation of BCL6 is ERK-independent.

Together, the results in Fig. 1 and Supplementary Figs 1–6 demonstrate that FBXO11 mediates the ubiquitylation and degradation of BCL6. As the levels of BCL6 are elevated in B-cell malignancies and increased BCL6 expression has a crucial role in the pathogenesis of DLBCL, we determined whether the loss of FBXO11 might account for the elevated levels of BCL6. We examined the expression of FBXO11 and BCL6 in 22 B-cell lymphoma cell lines, including 16 DLBCL cell lines. We found that FBXO11 was absent or expressed at low levels in three DLBCL cell lines (FARAGE, MHHPREB1 and HT), and the expression was inversely correlated with BCL6 expression (Supplementary Fig. 8a). Using quantitative real-time polymerase chain reaction (qRT–PCR) on genomic DNA, we found that the *FBXO11* gene was homozygously deleted in FARAGE and MHHPREB1 cells and hemizygously deleted in HT cells (Supplementary Fig. 8b, c). We then measured the stability of BCL6 in the 16 DLBCL cell lines by treating cells with either cycloheximide, which blocks protein synthesis, or etoposide, which enhances BCL6 degradation[8]. In some samples, UO126, a MEK inhibitor, was also added. First, we observed that treatment of cells with UO126 did not stabilize BCL6 (compare the 4-h time point with cycloheximide in the presence or absence of UO126 in Fig. 2), further supporting the conclusion that the FBXO11-mediated degradation of BCL6 is ERK-independent. Importantly, we found that in FARAGE, MHHPREB1 and HT cells, BCL6 was not only expressed at high levels, but it was also more stable than in other cell lines (Fig. 2).

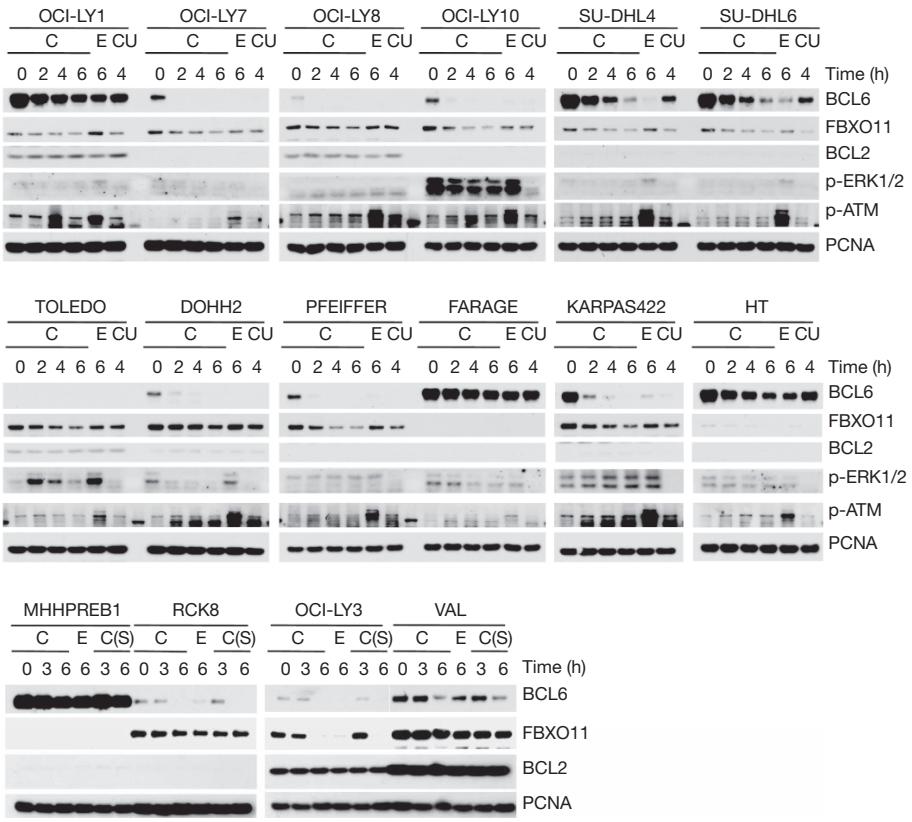

Figure 2 | DLBCL cell lines with *FBXO11* deletions or an *FBXO11* mutation display increased levels and stability of BCL6. Sixteen DLBCL cell lines were incubated with either cycloheximide (C), etoposide (E), or cycloheximide and UO126 (CU) for the indicated hours before immunoblotting for the indicated proteins. Where indicated, the intra S-phase (S) checkpoint was activated by incubating cells with thymidine for 20 h prior to treatment with cycloheximide.

Notably, the OCI-LY1 cell line also showed increased BCL6 stability, and sequencing of the *FBXO11* locus in OCI-LY1 cells revealed a point mutation in one of the CASH domains (Supplementary Fig. 9), the presumptive substrate recognition domains of FBXO11 (ref. 13).

We then used high-density, single nucleotide polymorphism (HD-SNP) genotyping in a cohort of 27 DLBCL cell lines and confirmed the presence of *FBXO11* deletions (including a focal deletion) in 14.8% of the samples (Supplementary Fig. 10). Public databases also indicate that the *FBXO11* locus is deleted in B-cell malignancies. For example, the GSK cancer cell line genomic profiling database shows that deletions in the *FBXO11* locus are present in six of 77 lymphoid cell lines, whereas only three of 255 non-lymphoid cell lines display *FBXO11* deletions (Supplementary Fig. 11). (Of these six lines, three are DLBCLs and one is a Burkitt's lymphoma.) Additionally, gene copy analyses in two different studies show *FBXO11* deletions in 6 of 69 primary DLBCLs (Supplementary Fig. 12) (refs 14, 15).

To investigate *FBXO11* gene inactivation in tumour samples further, we screened for mutations of *FBXO11* in 100 primary DLBCL samples (Supplementary Table 1). After filtering for known polymorphisms and synonymous mutations, potential inactivating mutations were further analysed and confirmed. This strategy identified a total of six sequence changes in four tumours, of which two were in the same codon (Supplementary Fig. 9). None of these four samples displayed either *BCL6* translocation or mutation of its promoter (Supplementary Table 2), and the analysis of paired normal DNA demonstrated the somatic origin of these events. Five of the six identified mutations are in the CASH domains, and one of these five changes creates a frame shift, resulting in chain termination and elimination of all three CASH domains. The fact that the point mutations are in highly conserved residues (Supplementary Fig. 9c) suggests that these FBXO11 mutants may be non-functional. Our analyses show that *FBXO11* is deleted (in most cases hemizygously) in 14.8% of DLBCL cell lines ($n = 27$) and

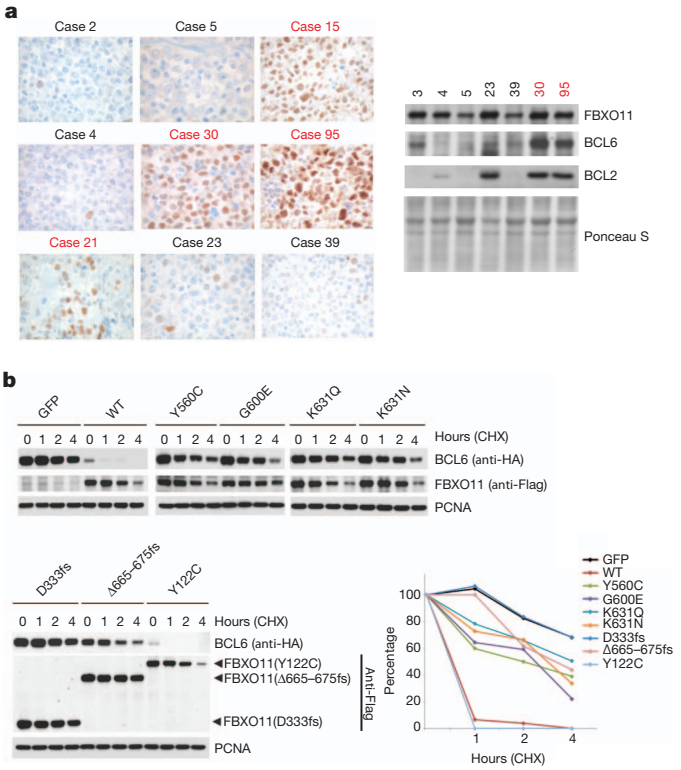

Figure 3 | Human DLBCLs with FBXO11 mutations display increased levels of BCL6, and FBXO11 tumour-derived mutants have impaired abilities to induce BCL6 degradation. **a**, Immunohistochemical stains for BCL6 from eight DLBCLs, including four tumours with mutations in *FBXO11*, are shown (brown) (×100). The right panel shows lysates from human DLBCLs that were analysed by immunoblotting for the indicated proteins. The red colour denotes DLBCL cases with *FBXO11* mutations. **b**, HEK-293T cells were transfected with BCL6 in combination with GFP, Flag-tagged wild type (WT) FBXO11, or the indicated Flag-tagged FBXO11 tumour-derived mutants. Twenty-four hours after transfection, cells were treated with cycloheximide (CHX) and samples were collected at the indicated time points for immunoblotting. The graph shows the quantification of BCL6 over the time course. The intensity of the bands from the experiment shown on the left was measured, and the ratio between the relative levels of BCL6 and PCNA in each time 0 was set as 100%.

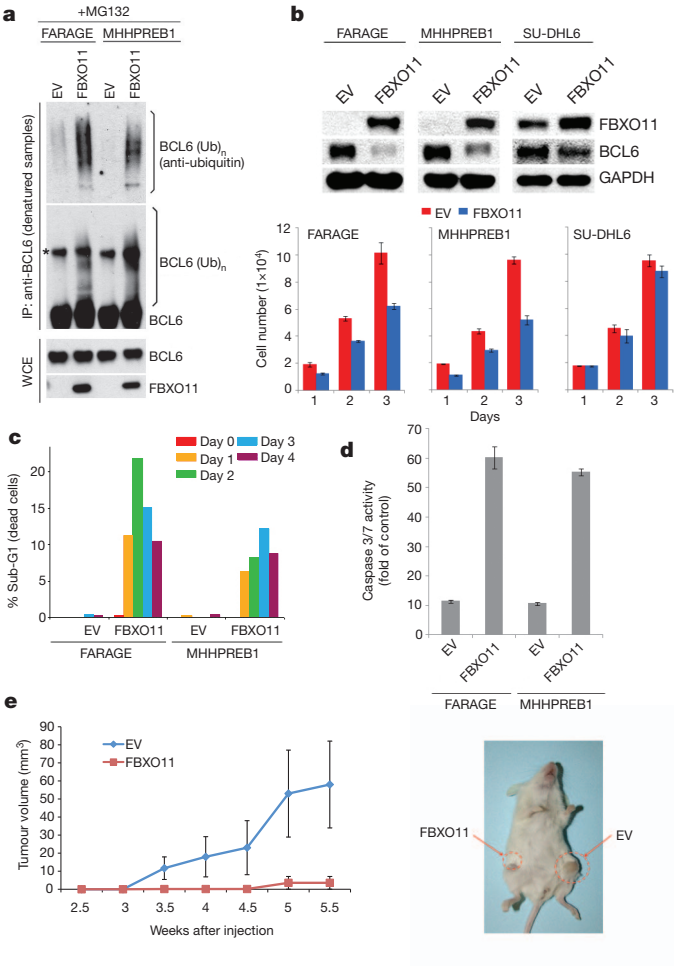

Figure 4 | Expression of FBXO11 in *FBXO11*-null cells promotes BCL6 ubiquitylation and degradation, inhibits cell proliferation and induces apoptosis. **a**, Denatured extracts from doxycycline- and MG132-treated FARAGE and MHHPREB1 cells stably transduced with a doxycycline-inducible FBXO11 construct or an empty virus (EV) were immunoprecipitated with an anti-BCL6 antibody and immunoblotted as indicated. The asterisk denotes a nonspecific band. Immunoblots of whole-cell extracts are also shown at the bottom. **b**, Extracts from doxycycline-treated FARAGE, MHHPREB1 and SU-DHL6 cells stably transduced with a doxycycline-inducible FBXO11 construct or an empty virus were immunoblotted as indicated. The graphs at the bottom show the number of cells measured in three different experiments (±s.d.) at different days after addition of doxycycline. **c**, Cells treated as in **b** for the indicated days were analysed by FACS. The graph represents the percentage of dying cells in the population (sub-G1 DNA content). **d**, Caspase 3 and Caspase 7 activity as measured in four different experiments (±s.d.) by the cleavage of a luminescent substrate in cells treated as in **b** for 2 days. The *y* axis indicates the caspase 3 and caspase 7 activity over cell number. The value given for the caspase activity in non-infected cells was set as 1. **e**, 1×10^7 FARAGE cells, stably transduced with a doxycycline-inducible FBXO11 construct (left flank) or an empty virus (right flank), were re-suspended in matrigel and injected subcutaneously into NOD/SCID mice. Two days after injection, doxycycline was administered in drinking water. Tumour growth was measured using a caliper at the indicated times after injection. $n = 4$ for each group; $P < 0.05$. Error bars indicate standard error of the mean (s.e.m.). The image on the right shows a representative mouse injected with the indicated cells.

mutated in 14.3% of DLBCL cell lines ($n = 7$) and 4% of primary DLBCLs ($n = 100$). Moreover, data available in public databases report *FBXO11* deletions in 8.7% of human DLBCLs ($n = 69$).

Notably, the DLBCL tumours with mutations in *FBXO11* expressed much higher BCL6 levels than control samples, as detected by immunohistochemistry (Fig. 3a). High BCL6 protein levels were also confirmed using immunoblotting when sufficient frozen tissue was available (Fig. 3a).

To investigate whether the *FBXO11* mutations in DLBCLs and OCI-LY1 cells interfere with FBXO11 activity, we generated complementary DNA constructs containing these mutations. Wild-type FBXO11 or FBXO11 mutants were expressed in HEK-293T cells to evaluate their ability to decrease BCL6 stability. Compared to wild-type FBXO11, tumour-derived FBXO11 mutants displayed an impaired ability to promote BCL6 degradation (Fig. 3b and Supplementary Fig. 13). Notably, FBXO11(Y122C), which has wild-type CASH domains, was the only mutant with activity similar to wild-type FBXO11. However, in the original sample this mutation was coupled with a deletion in FBXO11 that creates a frame shift and a chain termination (Δ666–675fs), which impaired the ability of FBXO11 to promote BCL6 degradation (Fig. 3b and Supplementary Fig. 13). We also found that mutations in FBXO11 modify its subcellular localization, preventing co-localization with BCL6 (Supplementary Fig. 14a, b). Moreover, FBXO11 mutants bind BCL6 less efficiently than wild-type FBXO11 (Supplementary Fig. 14c). These results indicate that the high levels of BCL6 observed in DLBCLs with FBXO11 mutations are due to a decreased ability of FBXO11 mutants to induce the proteolysis of BCL6.

To study the role of FBXO11 in tumorigenesis further, we used doxycycline-inducible retroviral expression vectors to express FBXO11 in two cell lines (FARAGE and MHHPREB1) with biallelic *FBXO11* deletion. BCL6 was poorly ubiquitylated in FARAGE and MHHPREB1 cells before FBXO11 reconstitution (Fig. 4a). Moreover, in parallel with a reduction in BCL6 levels, FBXO11 reconstitution inhibited cell proliferation in the *FBXO11*-null cell lines, but not a control line with an intact *FBXO11* locus (Fig. 4b). FBXO11 expression also induced apoptosis, as determined by a significant increase in the percentage of the sub-G1 population and activation of caspases 3 and 7 (Fig. 4c, d). Finally, FARAGE cells transduced with FBXO11 or an empty virus were injected subcutaneously into NOD/SCID mice. Induction of FBXO11 expression with doxycycline inhibited tumour growth, as revealed by measuring tumour mass (Fig. 4e).

Our results show that SCF^{FBXO11} is the ubiquitin ligase for BCL6 and that deregulation of this interaction may represent an oncogenic event. FBXO11 loss or mutation may contribute to DLBCL pathogenesis by allowing the accumulation of BCL6, an oncoprotein that has a critical role in lymphomagenesis. Because the deletions and mutations observed in our DLBCL samples were typically mono-allelic, we propose that FBXO11 is the product of a haplo-insufficient tumour suppressor gene.

METHODS SUMMARY

Biochemical methods. Extract preparation, immunoprecipitation and immunoblotting have previously been described[16]. Whole-cell lysates were generated by lysing cells in SDS lysis buffer (50 mM Tris pH 6.8, 2% SDS, 10% glycerol, 1 mM Na_3VO_4, 1 mM NaF and protease inhibitor mix (Roche)). *In vitro* ubiquitylation assays were preformed as described[16,17]. Briefly, haemagglutinin (HA)-tagged BCL6 was transfected into HEK-293T cells together with either Flag-tagged FBXO11 or an empty vector. Where indicated, MYC-tagged CUL1(1–242) was also transfected. Twenty-four hours after transfection, cells were incubated with MG132 for three hours before harvesting. Anti-Flag M2 agarose beads were used to immunoprecipitate the SCF^{FBXO11} complex. The beads were washed four times in lysis buffer and twice in ubiquitylation reaction buffer (10 mM Tris-HCl, pH 7.5, 100 mM NaCl, and 0.5 mM dithiothreitol). Beads were then used for *in vitro* ubiquitylation assays in a volume of 30 μl, containing 0.1 μM E1 (Boston Biochem), 0.25 μM Ubch3, 0.25 μM Ubch5c, 1 μM ubiquitin aldehyde, 2.5 μg μl^{-1} ubiquitin, and 1× magnesium/ATP cocktail. Samples were incubated for 2 h at 30 °C and analysed by immunoblotting. *In vivo* ubiquitylation assays were preformed as described[18].

Mutation analysis. The complete coding sequences and exon/intron junctions of *FBXO11* were analysed by PCR amplification and sequencing. The reference sequences for all annotated exons and flanking introns of *FBXO11* were obtained from the UCSC Human Genome database using the mRNA accession NM_025133.4. PCR primers (see Supplementary Table 3), located ≥50 bp upstream or downstream of the target exon boundaries, were designed in the Primer 3 program (http://frodo.wi.mit.edu/primer3/). Sequences were compared to the corresponding germline sequences using the Mutation Surveyor Version 2.41 software package (Softgenetics; http://www.softgenetics.com). Synonymous mutations, previously reported polymorphisms (Human dbSNP Database at NCBI, build 130, and Ensembl Database) and changes present in the matched normal DNA were excluded.

Full Methods and any associated references are available in the online version of the paper at www.nature.com/nature.

Received 21 March; accepted 28 October 2011.
Published online 23 November 2011; corrected 4 January 2012 (see full-text HTML version for details).

1. Ci, W., Polo, J. M. & Melnick, A. B-cell lymphoma 6 and the molecular pathogenesis of diffuse large B-cell lymphoma. *Curr. Opin. Hematol.* **15,** 381–390 (2008).
2. Staudt, L. M. & Dave, S. The biology of human lymphoid malignancies revealed by gene expression profiling. *Adv. Immunol.* **87,** 163–208 (2005).
3. Baron, B. W. *et al.* The human BCL6 transgene promotes the development of lymphomas in the mouse. *Proc. Natl Acad. Sci. USA* **101,** 14198–14203 (2004).
4. Cattoretti, G. *et al.* Deregulated BCL6 expression recapitulates the pathogenesis of human diffuse large B cell lymphomas in mice. *Cancer Cell* **7,** 445–455 (2005).
5. Cardozo, T. & Pagano, M. The SCF ubiquitin ligase: insights into a molecular machine. *Nature Rev. Mol. Cell Biol.* **5,** 739–751 (2004).
6. Skaar, J. R., D'Angiolella, V., Pagan, J. K. & Pagano, M. SnapShot: F Box Proteins II. *Cell* **137,** 1358 (2009).
7. Niu, H., Ye, B. H. & Dalla-Favera, R. Antigen receptor signaling induces MAP kinase-mediated phosphorylation and degradation of the BCL-6 transcription factor. *Genes Dev.* **12,** 1953–1961 (1998).
8. Phan, R. T., Saito, M., Kitagawa, Y., Means, A. R. & Dalla-Favera, R. Genotoxic stress regulates expression of the proto-oncogene Bcl6 in germinal center B cells. *Nature Immunol.* **8,** 1132–1139 (2007).
9. Benmaamar, R. & Pagano, M. Involvement of the SCF complex in the control of Cdh1 degradation in S-phase. *Cell Cycle* **4,** 1230–1232 (2005).
10. Piva, R. *et al. In vivo* interference with Skp1 function leads to genetic instability and neoplastic transformation. *Mol. Cell. Biol.* **22,** 8375–8387 (2002).
11. Yen, H. C. & Elledge, S. J. Identification of SCF ubiquitin ligase substrates by global protein stability profiling. *Science* **322,** 923–929 (2008).
12. Skaar, J. R. & Pagano, M. Control of cell growth by the SCF and APC/C ubiquitin ligases. *Curr. Opin. Cell Biol.* **21,** 816–824 (2009).
13. Jin, J. *et al.* Systematic analysis and nomenclature of mammalian F-box proteins. *Genes Dev.* **18,** 2573–2580 (2004).
14. Edgar, R., Domrachev, M. & Lash, A. E. Gene Expression Omnibus: NCBI gene expression and hybridization array data repository. *Nucleic Acids Res.* **30,** 207–210 (2002).
15. Kato, M. *et al.* Frequent inactivation of A20 in B-cell lymphomas. *Nature* **459,** 712–716 (2009).
16. D'Angiolella, V. *et al.* SCF(Cyclin F) controls centrosome homeostasis and mitotic fidelity through CP110 degradation. *Nature* **466,** 138–142 (2010).
17. Duan, S. *et al.* mTOR generates an auto-amplification loop by triggering the βTrCP- and CK1α-dependent degradation of DEPTOR. *Mol. Cell* **44,** 317–324 (2011).
18. Bloom, J., Amador, V., Bartolini, F., DeMartino, G. & Pagano, M. Proteasome-mediated degradation of p21 via N-terminal ubiquitinylation. *Cell* **115,** 71–82 (2003).

Supplementary Information is linked to the online version of the paper at www.nature.com/nature.

Acknowledgements We thank W. Carroll, S. Shaham and L. Staudt for sharing unpublished results; A. Melnick, Y. Sun and Y. Xiong for reagents; L. Cerchietti, Y. Cheng, E. Dehan, V. Donato, N. V. Dorello, S. N. Yang and Z. Yao for advice and/or contributions to this work. M.P. is grateful to T. M. Thor and K. E. Davidson, and L.C. to Zuzana S. for continuous support. This work was supported by grants from the National Institutes of Health to M.P. (R01-GM57587, R37-CA76584 and R21-CA161108) and M.S. (PO1-CA092625), a grant from Susan G. Komen for the Cure to S.D., a Lymphoma Research Foundation Fellowship to J.K.P. and grants from AIRC and ERC (ERC-2009-StG-Proposal No242965-LUNELY) to R.C. M.P. is an Investigator with the Howard Hughes Medical Institute.

Author Contributions S.D., L.C. and J.K.P. planned and performed most experiments and helped to write the manuscript. M.P. coordinated the study, oversaw the results and wrote the manuscript. C.M., P.F.d.C. and R.C. provided the DLBCL tumour samples and some DLBCL cell lines, and performed some experiments. M.R. generated several constructs. B.C. and M.S. provided the HD-SNP data in Supplementary Fig. 10. All authors discussed the results and commented on the manuscript.

Author Information Reprints and permissions information is available at www.nature.com/reprints. The authors declare no competing financial interests. Readers are welcome to comment on the online version of this article at www.nature.com/nature. Correspondence and requests for materials should be addressed to M.P. (michele.pagano@nyumc.org) or R.C. (roberto.chiarle@unito.it).

METHODS

Cell culture and drug treatments. With the exception of OCI-LY7 and OCI-LY10, which were maintained in Iscove's Modified Dulbecco's Medium, all other B-cell lines were grown in RPMI-1640 medium. SK-MEL-28, HeLa, U-2OS and HEK-293T cells were maintained in Dulbecco's Modified Eagle's Medium (DMEM). All media were supplemented with 10% fetal calf serum (FCS), 100 U ml^{-1} penicillin, 100 U ml^{-1} streptomycin and 2 mM L-glutamine. Where indicated, the following drugs were used: MG132 (10 μM), etoposide (20 μM) and cycloheximide (100 μg ml^{-1}).

Transient transfections. HEK-293T cells were transfected using polyethylenimine (PEI, Polysciences). HeLa, SK-MEL-28 and U-2OS cells were transfected using Lipofectamine 2000 (Invitrogen).

Gene silencing by siRNAs and shRNAs. All sequences of siRNAs and shRNAs are listed in Supplementary Table 3. shRNA lentiviruses were produced as described[8]. B cells were infected by re-suspension in the virus-containing supernatants and centrifugation. Twenty-four hours after infection, cells were re-suspended in fresh medium and selected with puromycin.

Antibodies. The following rabbit polyclonal antibodies were used: BCL6 (N-3; Santa Cruz Biotechnology), FBXO11 (Novus Bio), FBXO1 (C-20; Santa Cruz Biotechnology), FBXO5 (Invitrogen), FBXO31 (Bethyl), CUL1 (Invitrogen), FBXL1 (Invitrogen), BCL2 (C21; Santa Cruz Biotechnology), CDH1 (Invitrogen), CDC20 (Invitrogen), α-tubulin (Sigma), HA (Covance), Myc (Bethyl) and Flag (Sigma). Antibodies against FBXO18, FBXW9 and SKP1 were generated in the Pagano laboratory, and those to RBX1 were from Y. Xiong. Rabbit monoclonal antibodies were from Cell Signaling (FBXW1, GAPDH and phospho-ERK1/2 (Thr 202/Tyr 204)). The following mouse monoclonal antibodies were used: BCL6 (5G11; Santa Cruz Biotechnology), BCL6 (PG-B6p, Dako), BCL2 (C2; Santa Cruz Biotechnology), CD10 (56C6, Novocastra), pATM (S1981) (Cell Signaling), PCNA (PC10, Invitrogen), MUM1/IRF4 (MUM1p, Dako), p53 (DO-1, Santa Cruz Biotechnology), ubiquitin (Millipore) and β-actin (Sigma).

***In vitro* binding assay.** HA-tagged BCL6 was *in vitro* transcribed/translated using the TnT T3 Coupled Wheat Germ Extract System (Promega) and purified with anti-HA agarose (Roche). Bead-bound BCL6 was incubated with soluble Flag-tagged FBXO11 (purified from HEK293T cells), re-purified with HA agarose beads and subjected to immunoblotting. In some cases, bead-bound BCL6 was either treated with λ-phosphatase (NEB) or phosphorylated with ERK2 before extensive washing and incubation with Flag-tagged FBXO11. Kinase assays were performed by incubating bead-bound BCL6 at 30 °C for 1 h with 2.5 μCi [γ-^{32}P]-ATP, 2 mM ATP and 200 ng active, recombinant, purified ERK2 (Millipore) in 30 μl kinase buffer (10 mM MOPS, pH 7.6, 1× magnesium/ATP cocktail (Upstate), 10 mM $MnCl_2$, 1 mM dithiothreitol).

Apoptosis and *in vivo* assays. 1×10^5 FARAGE, MHHPREB1, or SU-DHL6 cells stably transduced with a tetracycline-inducible FBXO11 construct or an empty virus were seeded in the presence of doxycycline. Cells were collected at different days, washed in PBS, and fixed in 70% cold ethanol. Cell death was measured by propidium iodide staining and FACS. The percentage of sub-G1 phase cells was calculated using FlowJo software (FlowJo). Apoptosis was determined by measuring the activity of the caspases 3 and 7 using a luminescent substrate (Caspase-Glo 3/7; Promega). *In vivo* tumorigenicity assay was performed as described[15]. All animal procedures followed NIH protocols and were approved by the University Animal Institute Committee.

Immunofluorescence and immunohistochemistry. For indirect immunofluorescence staining, cells were grown on chamber slides, pre-extracted with CSK buffer (0.5% Triton X-100, 1 mM EDTA, 100 mM NaCl, 300 mM sucrose, 3 mM $MgCl_2$, 1 mM Na_3VO_4, 1 mM NaF, 2 mM $CaCl_2$, 10 mM HEPES pH 7.4) and fixed with 4% paraformaldehyde. Cells were permeabilized with PBS/0.2% Triton X-100 and blocked in PBS/0.1% Tween containing 3% BSA before incubation with primary antibodies. Alexa Fluor-conjugated 555 donkey anti-rabbit and Alexa Fluor 488-conjugated goat anti-mouse IgG were used as secondary antibodies. DAPI was used to counterstain DNA. Slides were mounted with Prolong-Gold (Invitrogen). Image acquisition was performed using a Zeiss Axiovert 200 M microscope, equipped with a cooled Retiga 2000R CCD (QImaging) and Metamorph Software (Molecular Devices). Immunohistochemistry was performed as described[19].

Intraperitoneal immunization and preparation of activated B cells. Sheep blood Alsevers (BD) were washed with PBS and re-suspended in PBS at a concentration of 1×10^9 sheep red blood cells (SRBCs) per ml. Mice were then immunized intraperitoneally with 2×10^8 SRBCs in a 200 μl volume. After 5 days, mice were immunized again using 5–10-fold more SRBCs. Spleens were collected 7–10 days after immunization, placed on ice, washed in PBS to remove residual blood, cut into small pieces, crushed, physically dissociated using a Falcon cell strainer, and subjected to hypotonic lysis of erythrocytes.

Preparation of genomic DNA. DNA from DLBCL samples was generated by proteinase K digestion and phenol-chloroform extraction. Genomic DNA from cell lines was prepared using QIAamp DNA kits (Qiagen).

Copy number determination by quantitative RT–PCR of genomic DNA. Genomic DNA was prepared using QIAamp DNA Kits (Qiagen). The DNA was amplified with Absolute Blue QPCR SYBR-Green Mix (Thermo Scientific) using a Light Cycler 480 System (Roche). Primers are listed in Supplementary Table 3. Normalization of gene copy number was performed with additional loci on chromosomes 5, 6 and 12. Genomic DNA from primary human diploid fibroblasts was used as a 2N DNA standard.

Quantitative RT–PCR of cDNA. Total RNA was prepared using RNeasy Kits (Qiagen) and treated with DNase I, and cDNA was generated by reverse transcription. The cDNA was amplified with Absolute Blue QPCR SYBR-Green Mix (Thermo Scientific) using a Light Cycler 480 System (Roche). Primers are listed in Supplementary Table 3. Normalization across samples was performed using the average gene expression of *SDHA*, *GAPDH* and *RPS13*.

Copy number determination by GEO database data analysis. The CEL files used for this study were obtained from the National Center for Biotechnology Information, Gene Expression Omnibus (http://www.ncbi.nlm.nih.gov/projects/geo). Raw data were processed, analysed and visualized using Genespring GX 11.5 software (Agilent).

19. Latres, E. *et al.* Role of the F-box protein Skp2 in lymphomagenesis. *Proc. Natl Acad. Sci. USA* **98,** 2515–2520 (2001).

doi:10.1038/nature10688

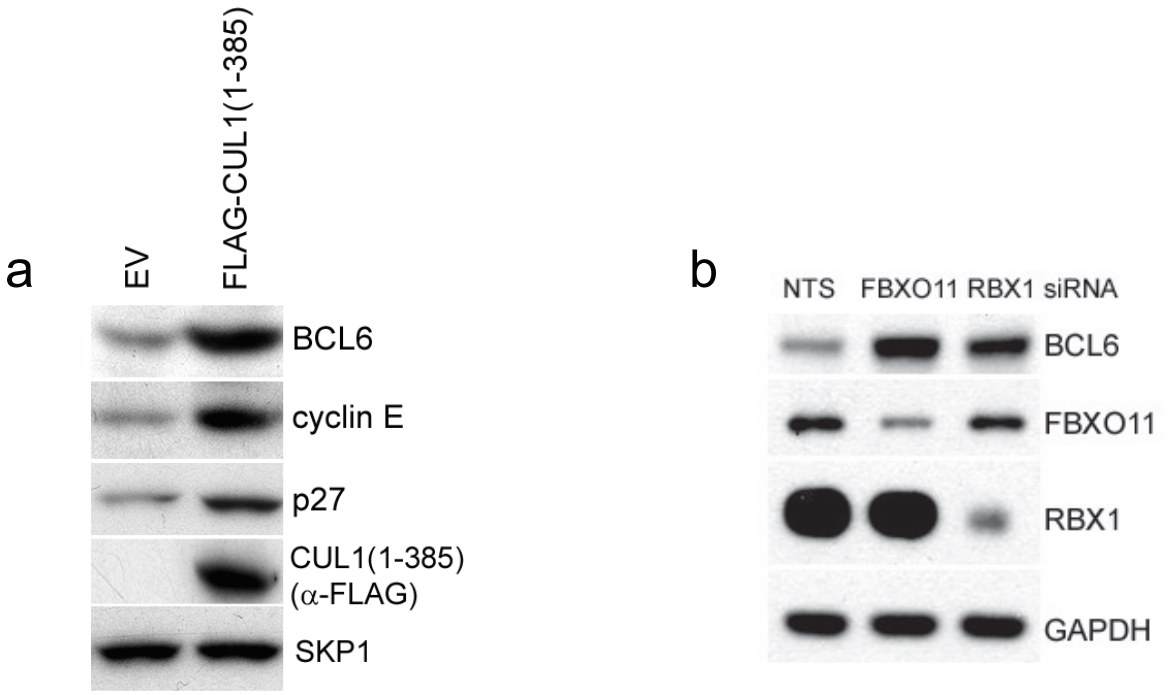

Supplementary Figure 1. BCL6 levels increase in response to the expression of a dominant negative CUL1 mutant or silencing of RBX1.

a, Ramos cells were infected with an empty virus (EV) or a virus expressing FLAG-tagged Cul1(1-385). Twenty-four hours post-infection, cells were harvested for immunoblotting as indicated. BCL6 levels increased in cells expressing Cul1(1-385), similar to p27 and cyclin E, two established SCF substrates[1-3].

b, SK-MEL-28 cells were transfected with either short interfering RNAs (siRNAs) to the indicated mRNAs or a non-targeting siRNA (NTS). Cells were collected 48 hours after transfection, lysed, and processed for immunoblotting with antibodies to the indicated proteins.

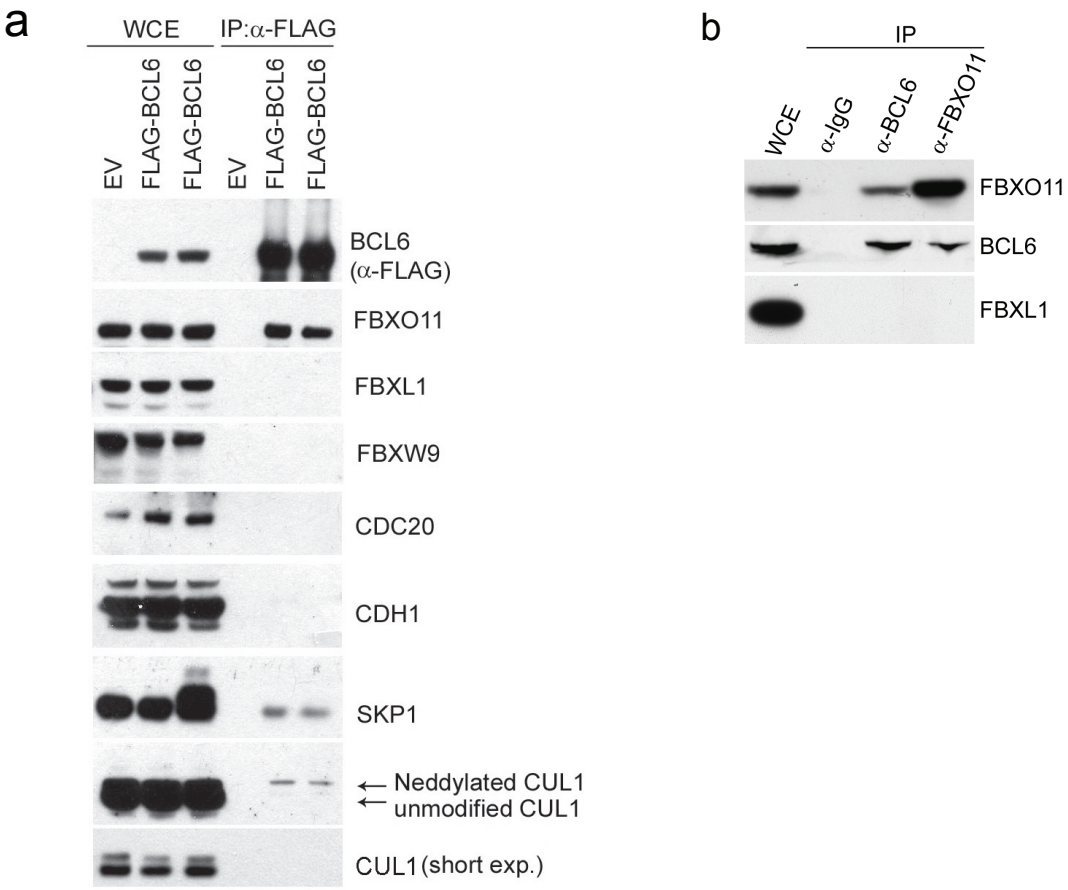

Supplementary Figure 2. BCL6 specifically interacts with FBXO11.

a, BCL6 specifically interacts with endogenous FBXO11. HEK-293T cells were transfected with FLAG-tagged BCL6 (in duplicate) or an empty vector (EV). Whole cell extracts (WCE) were immunoprecipitated (IP) with anti-FLAG resin and probed with antibodies to the indicated proteins. Exogenous BCL6 interacted with endogenous FBXO11, SKP1, and neddylated CUL1 (the form of CUL1 which preferentially binds SCF substrates), but not FBXL1, FBXW9, CDC20, or CDH1.

b, Endogenous FBXO11 and endogenous BCL6 associate in normal B-cells. B-cells from healthy immunized mice were treated with MG132 2.5 hours prior to lysis. Lysates were immunoprecipitated with either a polyclonal antibody against FBXO11, a polyclonal antibody to BCL6, or a nonspecific rabbit IgG and analyzed by immunoblotting as indicated.

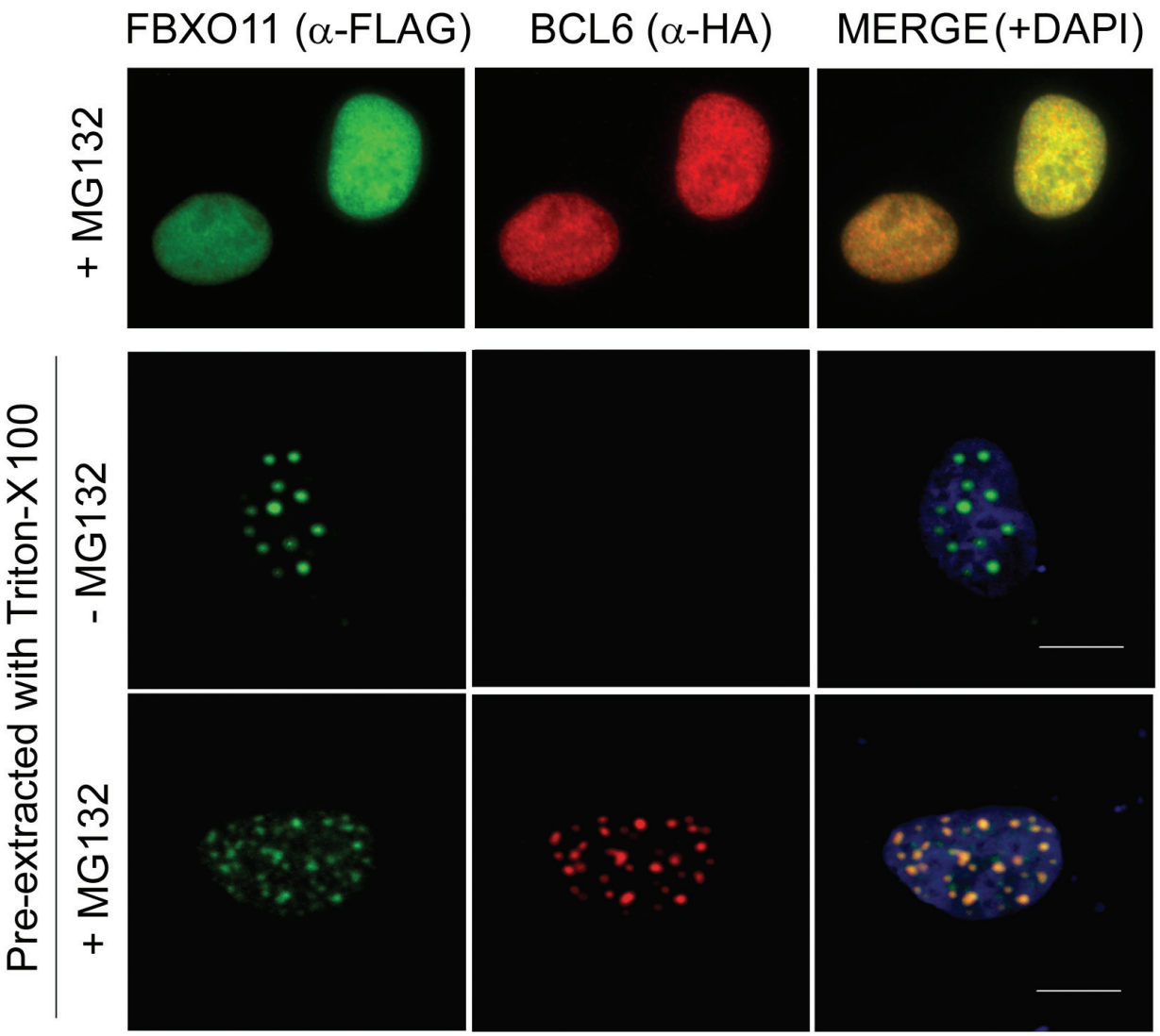

Supplementary Figure 3. BCL6 and FBXO11 colocalize in the nucleus.

U-2 OS cells were transfected with HA-tagged BCL6 and FLAG-tagged FBXO11. Twenty-four hours after transfection, cells were immunostained as indicated. Soluble nuclear proteins in the cells in the bottom panels were pre-extracted with 0.5% Triton-X100 prior to immunostaining. Where indicated, MG132 was added to prevent the degradation of BCL6. In the merged image, yellow shows colocalization of FBXO11 and BCL6. Both proteins were localized in the nucleus, but, after *in situ* cell fractionation, BCL6 and FBXO11 displayed an overlapping punctuate staining for throughout the nucleoplasm.

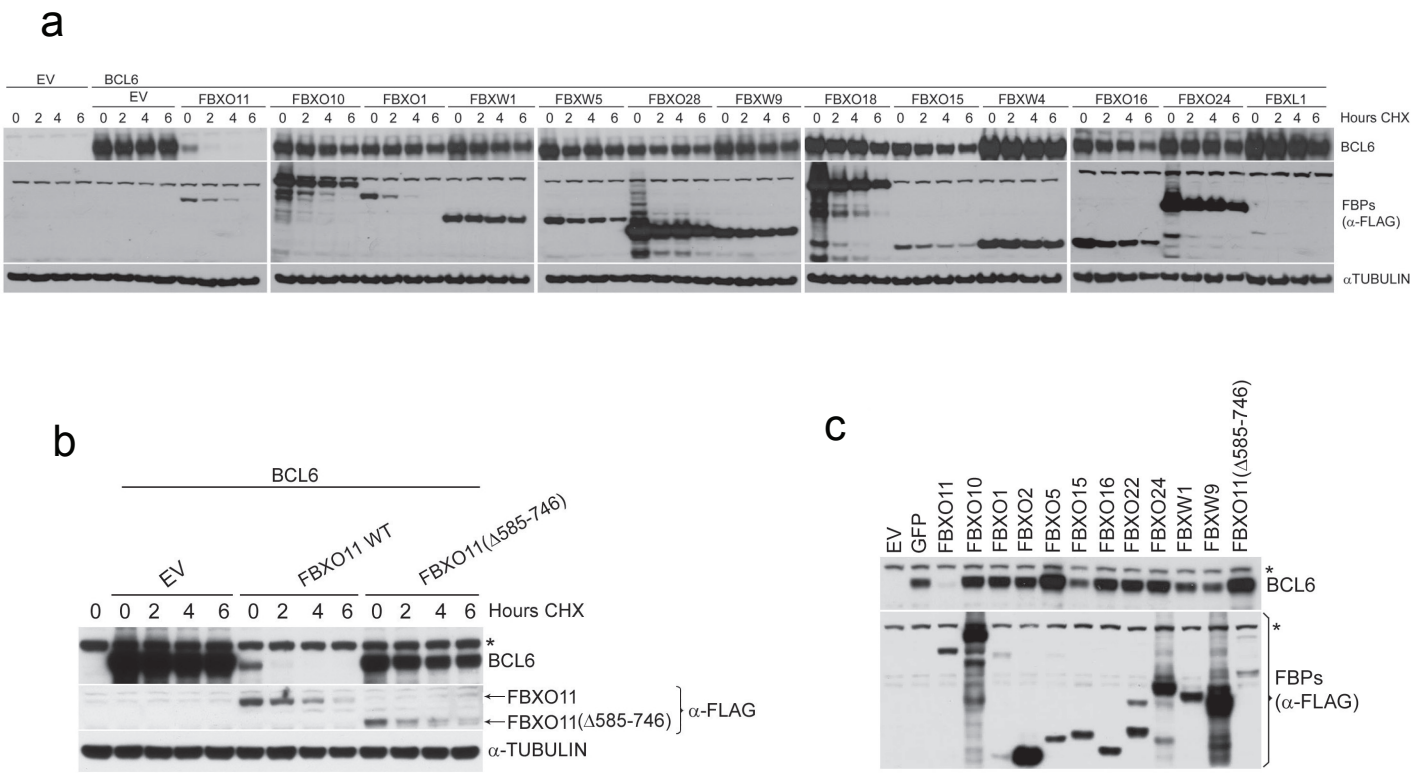

Supplementary Figure 4. Expression of FBXO11 induces a reduction in the levels and stability of BCL6.

a, FBXO11 is the only F-box protein that promotes efficient BCL6 degradation. HEK-293T cells were transfected with BCL6 in combination with either an empty vector (EV) or the indicated FLAG-tagged F-box proteins. Twenty-four hours post-transfection, cells were treated with cycloheximide (CHX), and samples were harvested at the indicated time points for immunoblotting. The lysates in the first four lanes are from cells transfected with EV alone.

b, FBXO11-mediated degradation of BCL6 requires the presumptive substrate recognition domain in FBXO11. HEK-293T cells were transfected with BCL6 in combination with either an empty vector (EV), FLAG-tagged FBXO11, or FLAG-tagged FBXO11(Δ585-746), an FBXO11 mutant missing the third of three CASH domains, the presumptive substrate recognition domains of FBXO11. Twenty-four hours post-transfection, cells were treated with cycloheximide (CHX), and samples were harvested at the indicated time points for immunoblotting. The lysate shown in the first lane is from untransfected cells. The asterisk denotes a non-specific band present in the anti-BCL6 blot. FBXO11(Δ585-746) was unable to induce BCL6 degradation, in agreement with its inability to bind BCL6 (as shown in Fig. 1A).

c, FBXO11 is the only F-box protein that promotes a reduction in BCL6 levels. HEK-293T cells were transfected with BCL6 alone or in combination with either an empty vector (EV), GFP, or the indicated FLAG-tagged F-box proteins. Twenty-four hours after transfection, cells were harvested, lysed, and processed for immunoblotting as indicated. The lysate in the first lane is from cells transfected with EV alone. The asterisks denote non-specific bands.

a

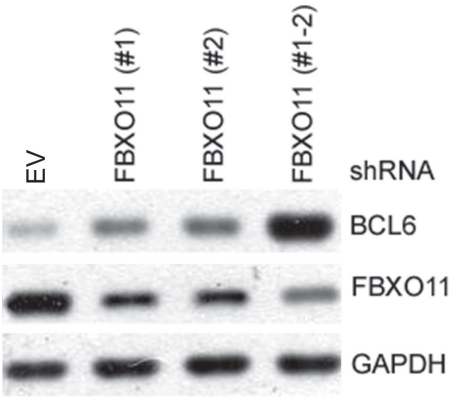
EV
FBXO11 (#1)
FBXO11 (#2)
FBXO11 (#1-2)
shRNA
BCL6
FBXO11
GAPDH

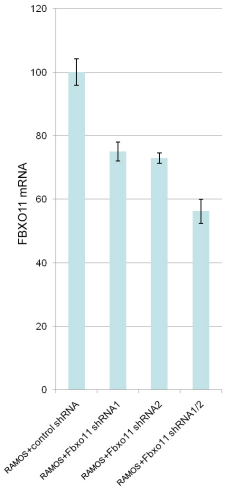
FBXO11 mRNA
120
100
80
60
40
20
0
RAMOS+control shRNA
RAMOS+Fbxo11 shRNA1
RAMOS+Fbxo11 shRNA2
RAMOS+Fbxo11 shRNA1/2

b

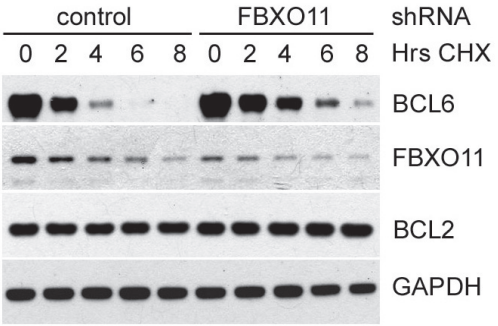
control
FBXO11
shRNA
0 2 4 6 8 0 2 4 6 8
Hrs CHX
BCL6
FBXO11
BCL2
GAPDH

c

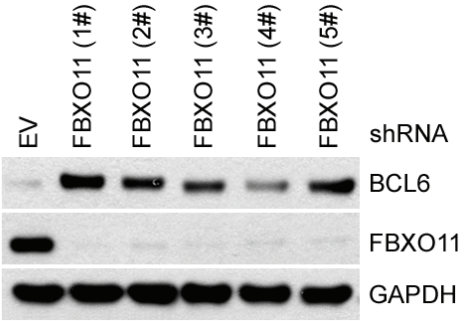
EV
FBXO11 (1#)
FBXO11 (2#)
FBXO11 (3#)
FBXO11 (4#)
FBXO11 (5#)
shRNA
BCL6
FBXO11
GAPDH

d

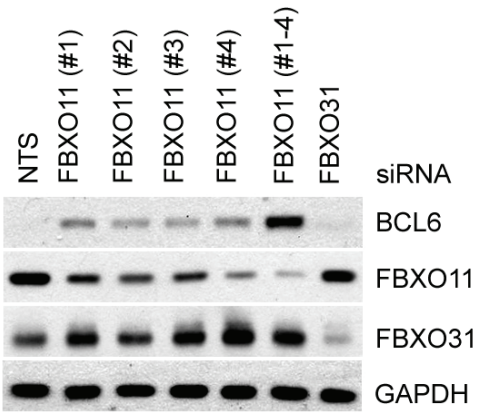
NTS
FBXO11 (#1)
FBXO11 (#2)
FBXO11 (#3)
FBXO11 (#4)
FBXO11 (#1-4)
FBXO31
siRNA
BCL6
FBXO11
FBXO31
GAPDH

e

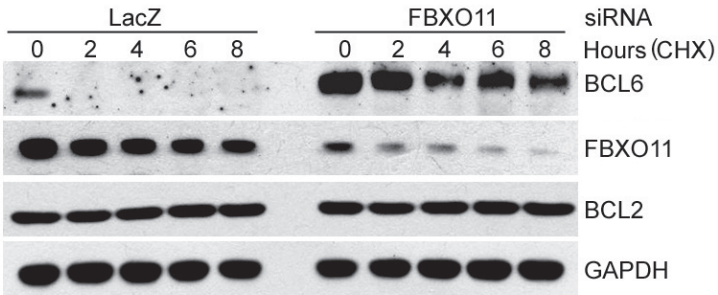
LacZ
FBXO11
siRNA
0 2 4 6 8 0 2 4 6 8
Hours (CHX)
BCL6
FBXO11
BCL2
GAPDH

Supplementary Figure 5. Silencing of *FBXO11* results in increased levels and stability of BCL6.

a, Ramos cells were infected with either viruses expressing two different *FBXO11* shRNAs (alone or in combination) or an empty virus (EV), and selected for 72 hours. Protein extracts were then immunoblotted for the indicated proteins. The bottom panel shows the analysis of *FBXO11* mRNA by quantitative Real-Time PCR in triplicate measurements (±SD). The amount of *FBXO11* mRNA present in the sample treated with the control shRNA was set as 100. Although both constructs alone targeted *FBXO11*, the combination of both was more efficient in silencing *FBXO11* expression. Accordingly, the combination of both constructs produced a more robust effect on BCL6 levels.

b, Ramos cells were infected with either viruses expressing two different *FBXO11* shRNAs (in combination) or an empty virus (EV), selected, and treated with cycloheximide for the indicated times. Protein extracts were immunoblotted for the indicated proteins.

c, SK-MEL-28 cells were infected with either viruses expressing five different *FBXO11* shRNAs or an empty virus (EV), and selected for 72 hours. Protein extracts were immunoblotted for the indicated proteins. [SK-MEL-28 melanoma cells express *BCL6* mRNA (http://biogps.gnf.org/#goto=genereport&id=604), in line with the evidence that BCL6 expression is not limited to the B-cell compartment. Indeed, primary melanocytes also express *BCL6* mRNA[4], and high levels of the BCL6 is associated with shorter survival in melanoma patients[5].]

d, SK-MEL-28 cells were transfected with either short interfering RNAs (siRNAs) to the indicated mRNAs (using four different oligos, alone or in combination for *FBXO11*) or a non-targeting siRNA (NTS). Cells were collected 48 hours after transfection, lysed, and processed for immunoblotting with antibodies to the indicated proteins. Although each of the four oligos induced FBXO11 downregulation alone, a pool of all four was more efficient in silencing FBXO11 expression and produced a more robust effect on BCL6 levels.

e, SK-MEL-28 cells were transfected with siRNAs to either a non-relevant mRNA (*LacZ*) or *FBXO11* mRNA (using a combination of four different oligos). Cells were treated with cycloheximide for the indicated times. Protein extracts were immunoblotted for the indicated proteins.

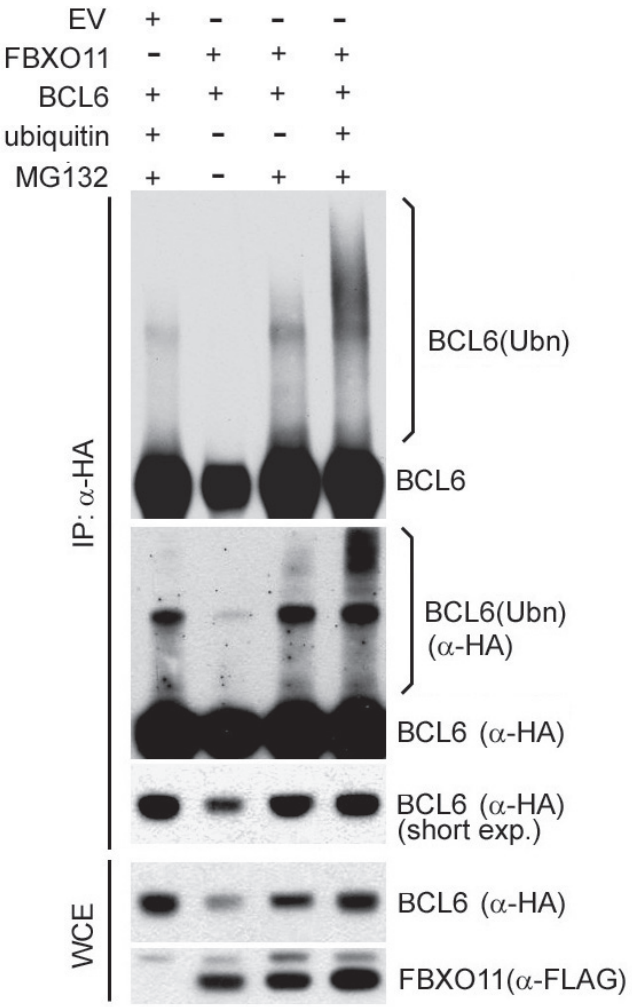

Supplementary Figure 6. FBXO11 promotes BCL6 ubiquitylation *in vivo*. HeLa cells were transfected with the indicated constructs and treated with MG132 as indicated. Whole cell extracts were denatured, immunoprecipitated with an anti-HA antibody (α-HA), and immunoblotted as indicated. The bracket on the left side of the top two panels marks a ladder of bands >86 kDa that corresponds to ubiquitylated BCL6.

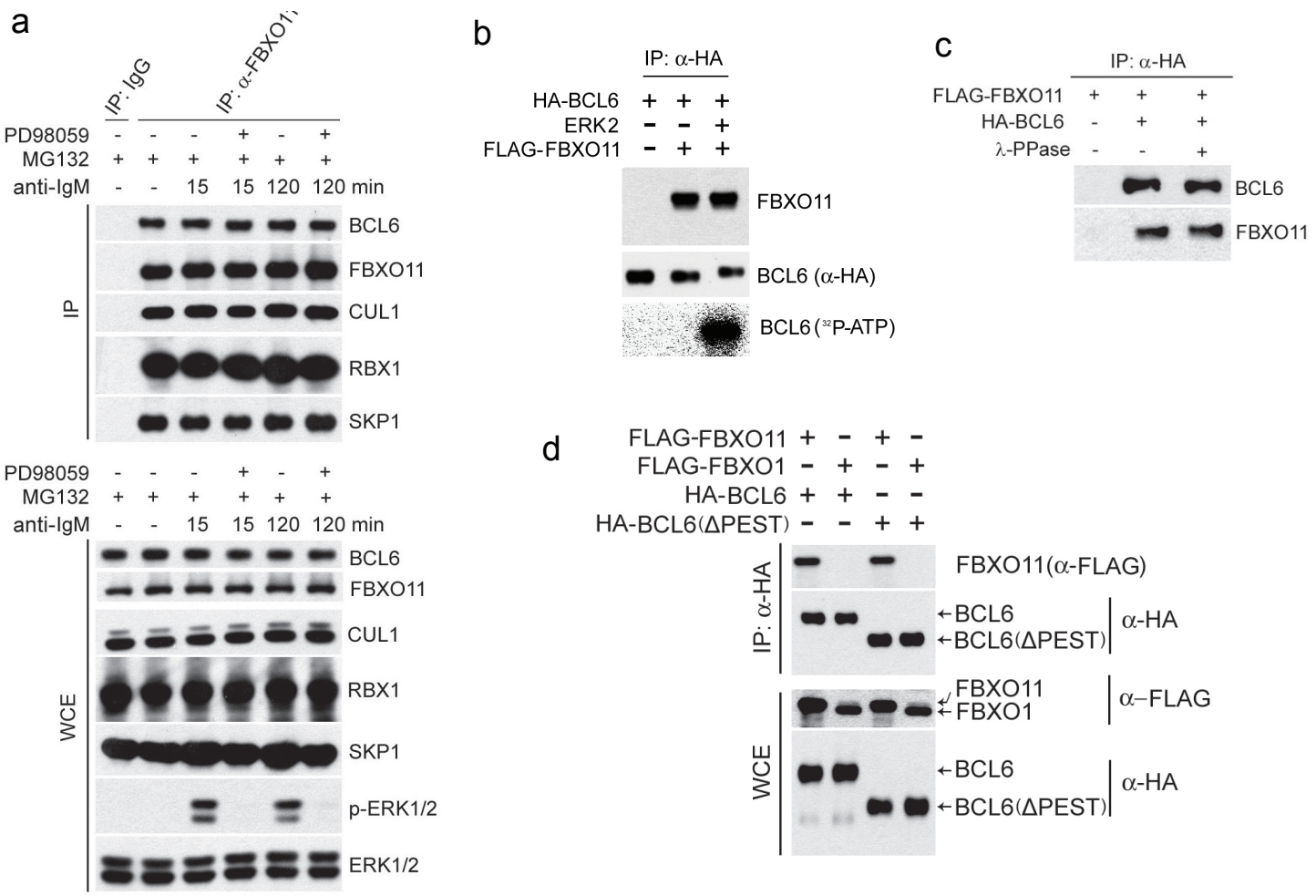

Supplementary Figure 7. FBXO11 binding to BCL6 is independent of B-cell antigen-receptor signaling and the MAPK pathway.

a, Ramos cells were incubated with anti-IgM antibodies [a treatment that mimics B-cell antigen-receptor signaling and activates ERK2 (ref[6])] in the presence of MG132 and in the presence or absence of PD98059, a MEK inhibitor, as indicated. Cells were lysed and extracts were immunoprecipitated with an anti-FBXO11 antibody. Immunoprecipitates and whole cell extracts (WCE) were immunoblotted for the indicated proteins.

b, *In vitro* transcribed/translated, HA-tagged BCL6 was purified with anti-HA agarose and subjected to a kinase reaction in the presence or absence of purified ERK2 using [γ-^{32}P]-ATP. BCL6 was then incubated with purified FLAG-FBXO11, re-purified with anti-HA agarose, and subjected to immunoblotting as indicated (top two panels). Only when incubated with ERK2, BCL6 displayed a gel shift, indicating that the majority of BCL6 was phosphorylated. The bottom panel shows a PhosphorImaging analysis of the kinase reaction product confirming that BCL6 is phosphorylated by ERK2.

c, *In vitro* transcribed/translated, HA-tagged BCL6 was purified with anti-HA agarose and treated with λ-phosphatase. (This λ-phosphatase treatment inhibited the binding of FBXW11 to one of its established substrates; not shown) BCL6 was then incubated with *in vitro* transcribed/translated FLAG-FBXO11, repurified with anti-HA agarose, and subjected to immunoblotting as indicated.

d, HEK-293T cells were transfected with either HA-tagged BCL6 or HA-tagged BCL6(ΔPEST), a mutant lacking amino acids 300-417, together with either FLAG-FBXO11 or FLAG-FBXO1, as indicated. Cells were treated with MG132 during the last five hours prior to harvest. Whole cell lysates (WCE) were purified with anti-HA agarose, and subjected to immunoblotting as indicated.

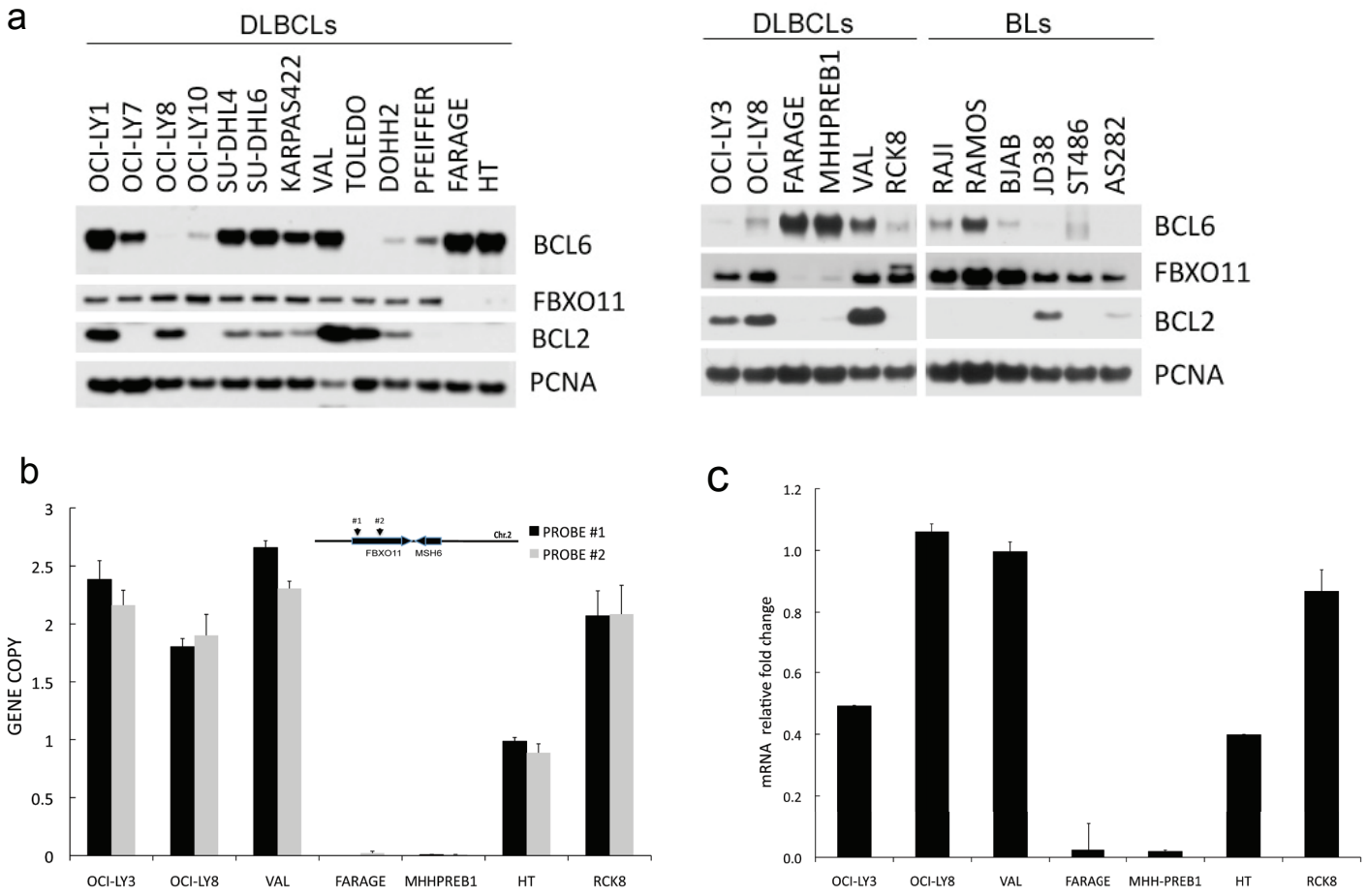

Supplementary Figure 8. ***FBXO11*** **is homozygously deleted in FARAGE and MHHPREB1 cells and hemizygously deleted in HT cells.**

a, Sixteen DLBCL cell lines and six Burkitt's lymphoma cell lines (BL) were analyzed by immunoblotting for the indicated proteins.

b, The histograms illustrate the mean value ratios of a quantitative Real Time-PCR (qRT-PCR) analysis of *FBXO11* gene copy number. The C_t values for two independent primer sets (depicted in the figure, see also Supplementary Table 3) were normalized using the median of gene copy numbers obtained with specific primers for loci on chromosomes 5, 6, and 12. The results are expressed as the amount of *FBXO11* DNA relative to these loci and are compared to the ratio found in primary human fibroblasts. The standard deviations were calculated from two experiments performed in duplicate.

c, The histograms illustrate the mean value ratios of a qRT-PCR analysis of *FBXO11* mRNA. The results are expressed as the amount of *FBXO11* mRNA relative to three housekeeping genes (*SDHA*, *GAPDH*, and *RPS13*). The amount of *FBXO11* mRNA present in VAL cells was set as 1.

a

OCI-LY1: Y560C

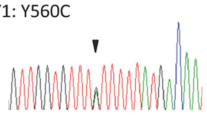

WT: GTTGGTGTTTATTTTTATGACAA
Val-Gly-Val-Tyr-Phe-Tyr-Asp
OCI-LY1: GTTGGTGTTTGTTTTTATGACAA
Val-Gly-Val-Cys-Phe-Tyr-Asp

CASE#15: Y122C

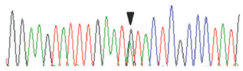

WT: GGAAGTATTTGAATATACTCGCCCTAT
Glu-Val-Phe-Glu-Tyr-Thr-Arg-Pro-Met
CASE#15: GGAAGTATTTGAATGTACTCGCCCTAT
Glu-Val-Phe-Glu-Cys-Thr-Arg-Pro-Met

CASE#15: Δ665-675*fs*

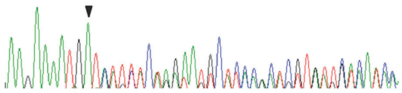

WT: AAGAAAATGATATTTTCAGGAATGCTCAAGCAGGTGTTCTCATCA
Glu-Glu-Asn-Asp-Iso-Phe-Arg-Asn-Ala-Gln-Ala-Gly-Val-Leu-Iso
CASE#15: AAGAAAATG-ATCAGCACTAA
Glu-Glu-Asn-Asp-Gln-His-Stop

CASE#21: D333*fs*

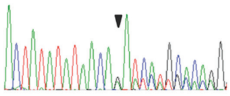

WT: ACTATATATAACAGATCATGCACAGG
Leu-Tyr-Iso-Thr-Asp-His-Ala-Gln-Gly
CASE#21: ACTATATATAACAAAATCATGCACAG
Leu-Tyr-Iso-Thr-Lys-Ser-Cys-Gln-Gly

CASE#21: K631Q

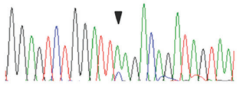

WT: GGAGTCTGGATTAAGACAGATAGTAA
Gly-Vall-Trp-Iso-Lys-Thr-Asp-Ser-Asn
CASE#21: GGAGTCTGGATTCAGACAGATAGTAA
Gly-Vall-Trp-Iso-Gln-Thr-Asp-Ser-Asn

CASE#30: G600E

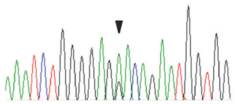

WT: AAATCTGGGGAGGACAGAATGGTGG
Lys-Iso-Trp-Gly-Gly-Gln-Asp-Gly-Gly
CASE#30: AAATCTGGGGAGAACAGAATGGTGG
Lys-Iso-Trp-Gly-Glu-Gln-Asp-Gly-Gly

CASE#95: K631N

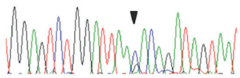

WT: GGAGTCTGGATTAAGACAGATAGTAA
Gly-Val-Trp-Iso-Lys-Thr-Asp-Ser
CASE#95: GGAGTCTGGATTAACACAGATAGTAA
Gly-Val-Trp-Iso-Asn-Thr-Asp-Ser

b

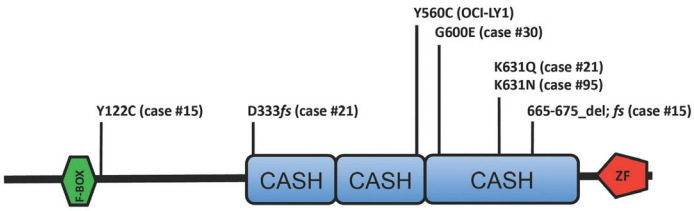

c

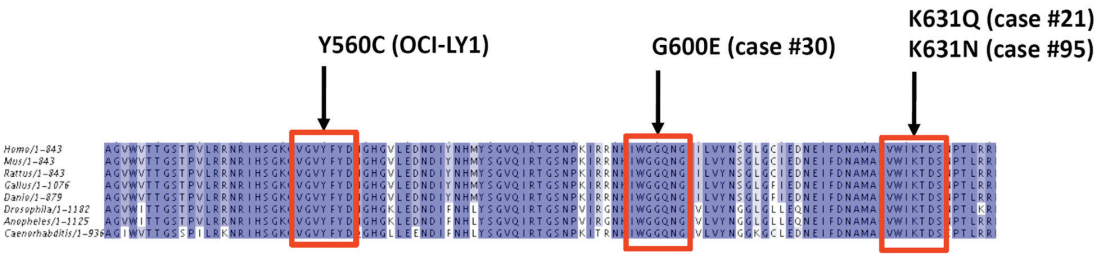

Supplementary Figure 9. *FBXO11* is mutated in OCI-LY1 cells and primary DLBCLs.

a, The chromatograms display *FBXO11* mutations (indicated by an arrow) identified by sequencing of RT-PCR products from the genomes of OCI-LY1 cells or the indicated DLBCLs (see Supplementary Table 1). Genomic DNA from six other DLBCL cell lines (OCI-LY3, OCI-LY8, SUDHL6, HT, RCK8, and VAL) was also sequenced, but no mutations in *FBXO11* were identified.

b, Mutations found in human DLBCLs are indicated above the domain structure of human FBXO11. In parenthesis, tumor numbers are indicated (see Table 1).

c, The amino acids changed in FBXO11 in OCI-LY1 cells and primary DLBCLs are conserved from worms to humans. The figure shows the alignment of the region in FBXO11 (from different species) that contains the amino acids changed in OCI-LY1 cells and primary DLBCLs. The red frame indicates the three amino acids found mutated in tumors.

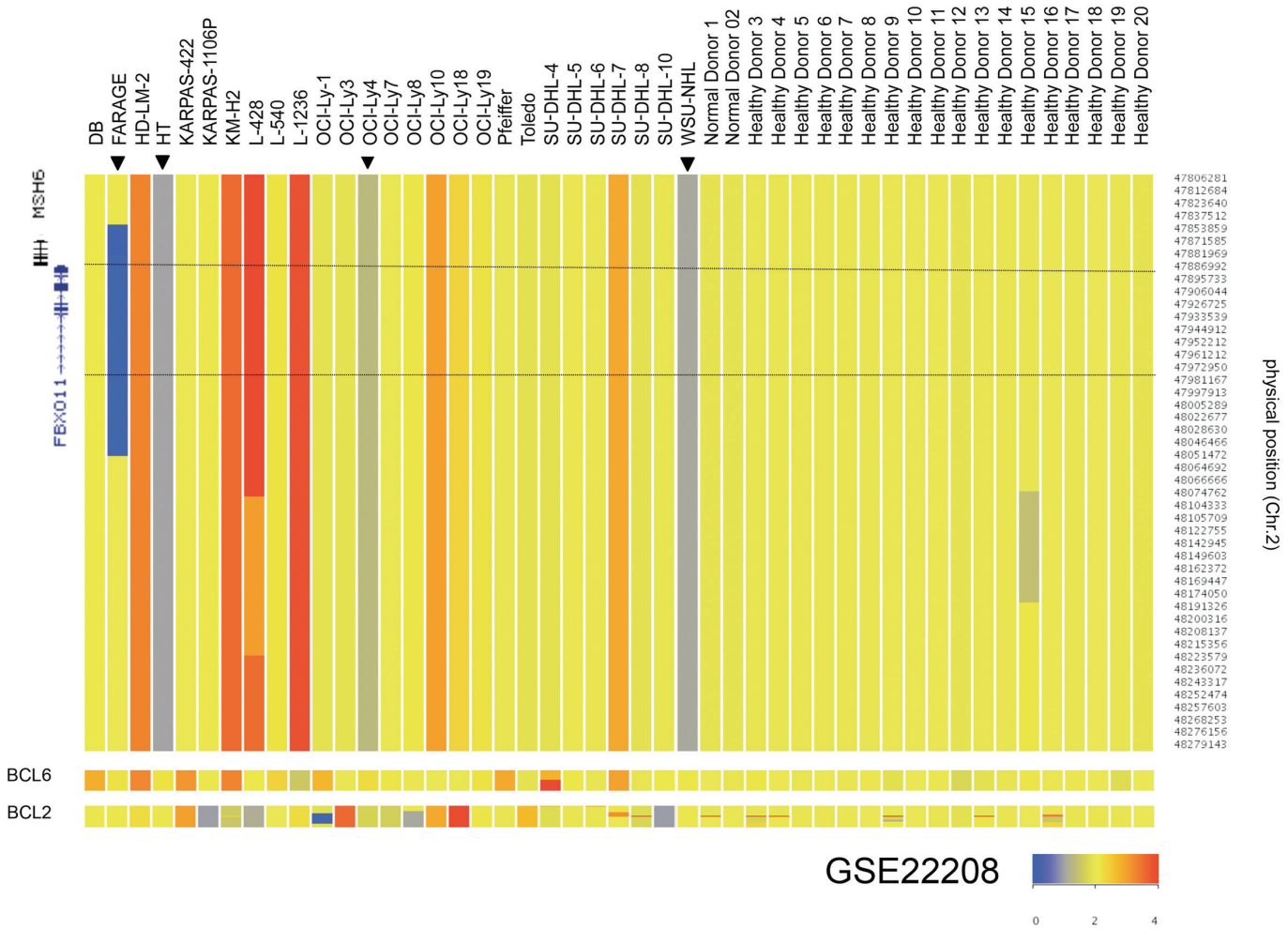

Supplementary Figure 10. The *FBXO11* gene is deleted in DLBCL cell lines.

Affymetrix Genome-Wide Human HD-SNP 6.0 array copy number data of the *FBXO11* locus in 27 DLBCL cell lines and 20 healthy donors is shown. The status of the *BCL6* and *BCL2* loci is also shown. The data are also accessible at the National Center for Biotechnology Information-Gene Expression Omnibus (NCBI-GEO; http://www.ncbi.nlm.nih.gov/geo/) database[7], accession # GSE22208 (ref [8]).

a

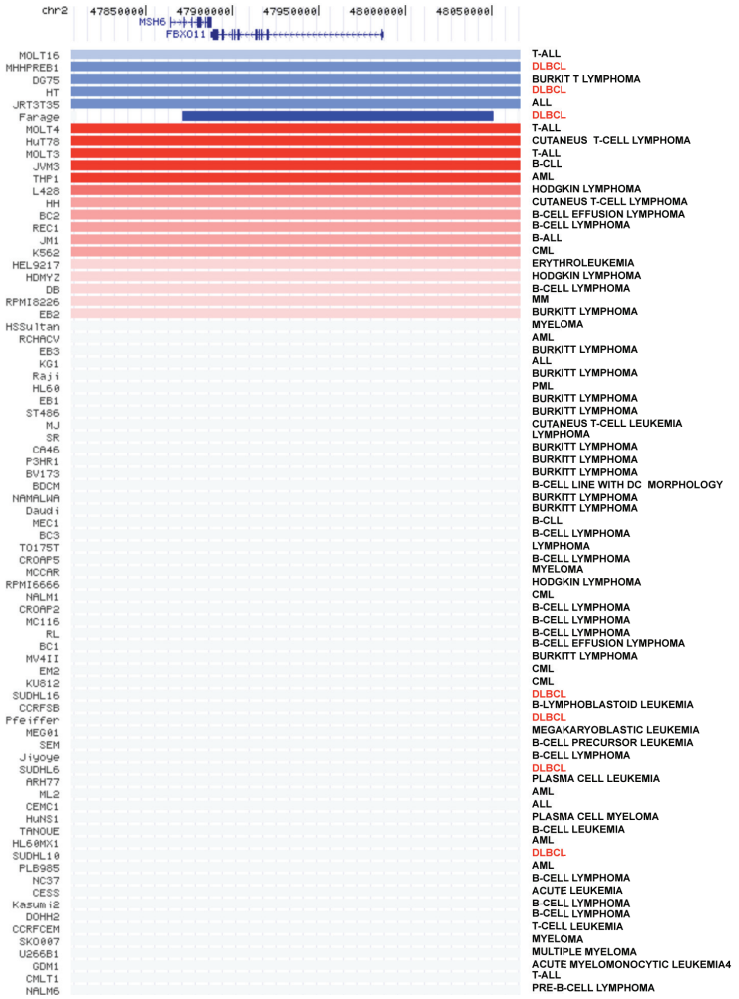

TISSUE (CELL LINE ORIGIN)	SAMPLES #	DEL.#
HEMATOPOIETIC	**77**	**6 (8%)**
- DLBCL	**7**	**3 (43%)**
NON-HEMATOPOIETIC	**255**	**3 (1%)**
BLADDER	10	0
BRAIN	7	1
BREAST	21	0
CNS	11	0
CERVIX	7	0
COLON	19	0
CONNECTIVE T.	4	0
ESOPHAGUS	4	0
EYE	1	0
KIDNEY	8	0
LIVER	9	0
LUNG	81	1
MUSCLE	4	0
OVARY	7	0
PANCREAS	9	0
PHARYNX	2	0
PLACENTA	3	0
PROSTATE	6	1
RECTUM	2	0
SARCOME	2	0
SKIN	12	0
STOMACH	5	0
SYNOVIUM	1	0
THYROIS	4	0
UTERUS	9	0
VULVA	3	0

b

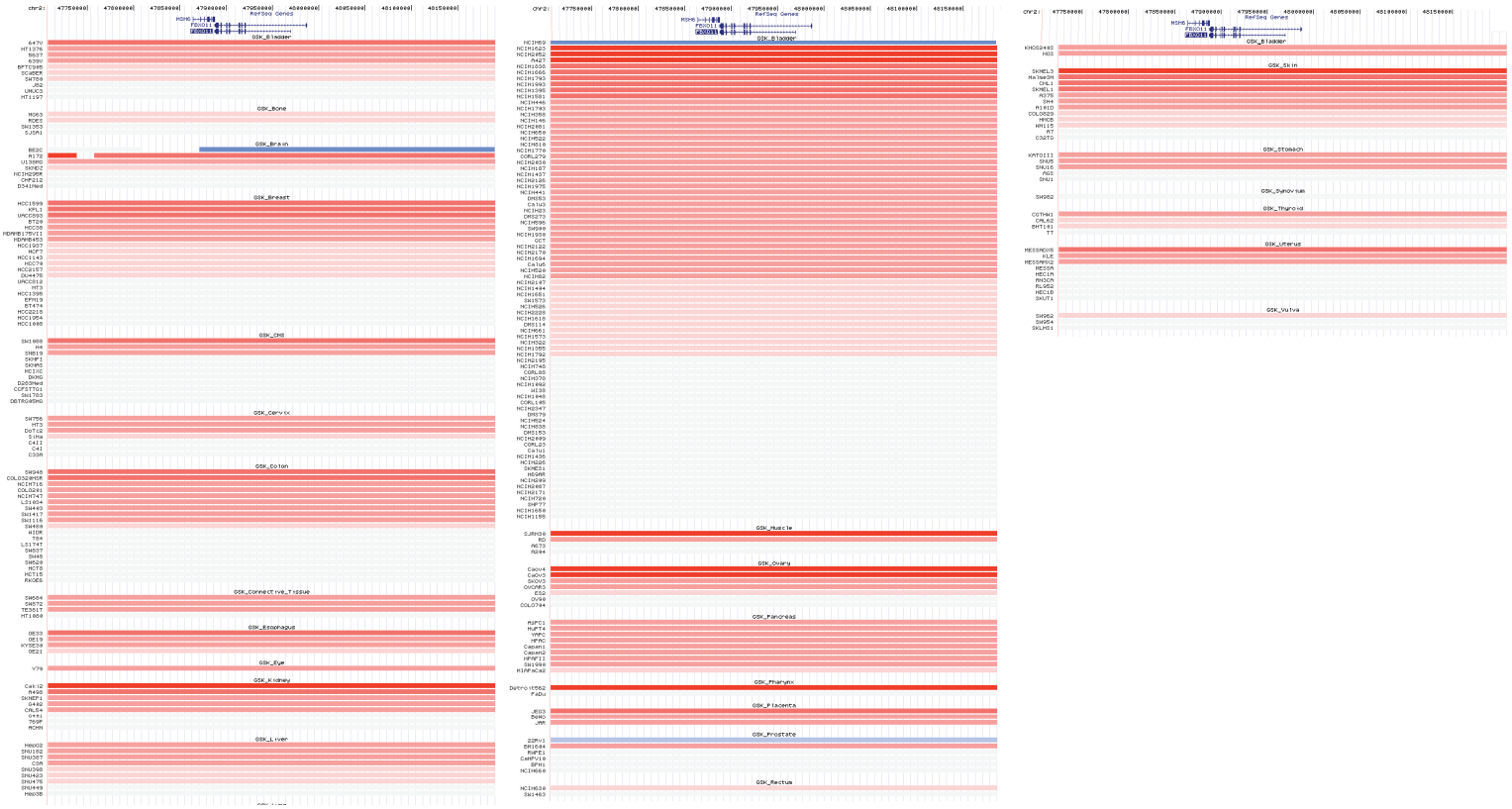
chr2:
47750000
47800000
47850000
47900000
47950000
48000000
48050000
48100000
48150000
RefSeq Genes
MSH6
FBXO11
GSK_Bladder
GSK_Bone
GSK_Brain
GSK_Breast
GSK_CNS
GSK_Cervix
GSK_Colon
GSK_Connective_Tissue
GSK_Esophagus
GSK_Eye
GSK_Kidney
GSK_Liver
GSK_Muscle
GSK_Ovary
GSK_Pancreas
GSK_Pharynx
GSK_Placenta
GSK_Prostate
GSK_Rectum
GSK_Skin
GSK_Stomach
GSK_Synovium
GSK_Thyroid
GSK_Uterus
GSK_Vulva

C

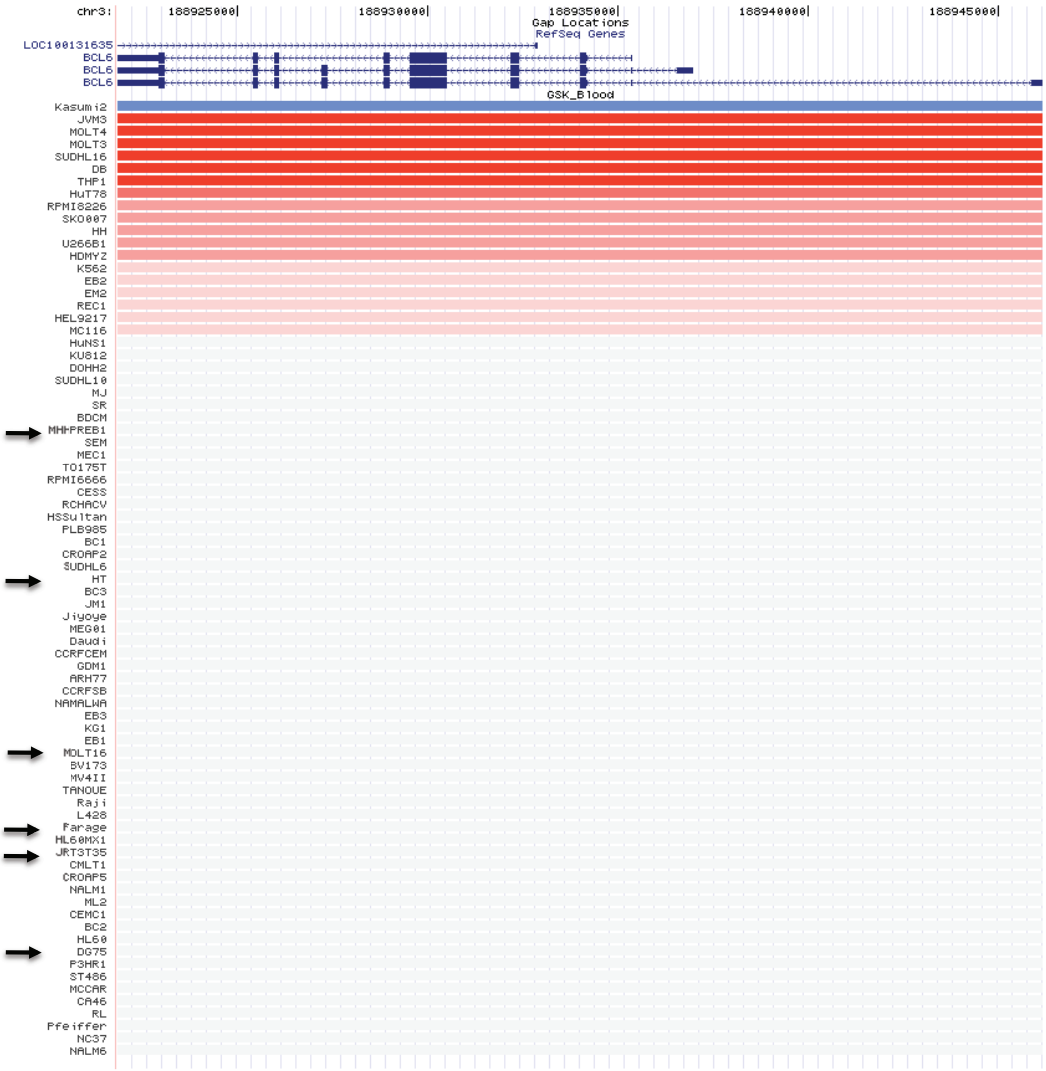
chr3:
188925000
188930000
188935000
188940000
188945000
Gap Locations
RefSeq Genes
LOC100131635
BCL6
BCL6
BCL6
GSK_Blood
Kasumi2
JVM3
MOLT4
MOLT3
SUDHL16
DB
THP1
HuT78
RPMI8226
SKO007
HH
U266B1
HDMYZ
K562
EB2
EM2
REC1
HEL9217
MC116
HuNS1
KU812
DOHH2
SUDHL10
MJ
SR
BDCM
MHHPREB1
SEM
MEC1
TO175T
RPMI6666
CESS
RCHACV
HSSultan
PLB985
BC1
CROAP2
SUDHL6
HT
BC3
JM1
Jiyoye
MEG01
Daudi
CCRFCEM
GDM1
ARH77
CCRFSB
NAMALWA
EB3
KG1
EB1
MOLT16
BV173
WV4II
TANOUE
Raji
L428
Farage
HL60MX1
JRT3T35
CMLT1
CROAP5
NALM1
ML2
CEMC1
BC2
HL60
DG75
P3HR1
ST486
MCCAR
CA46
RL
Pfeiffer
NC37
NALM6

d

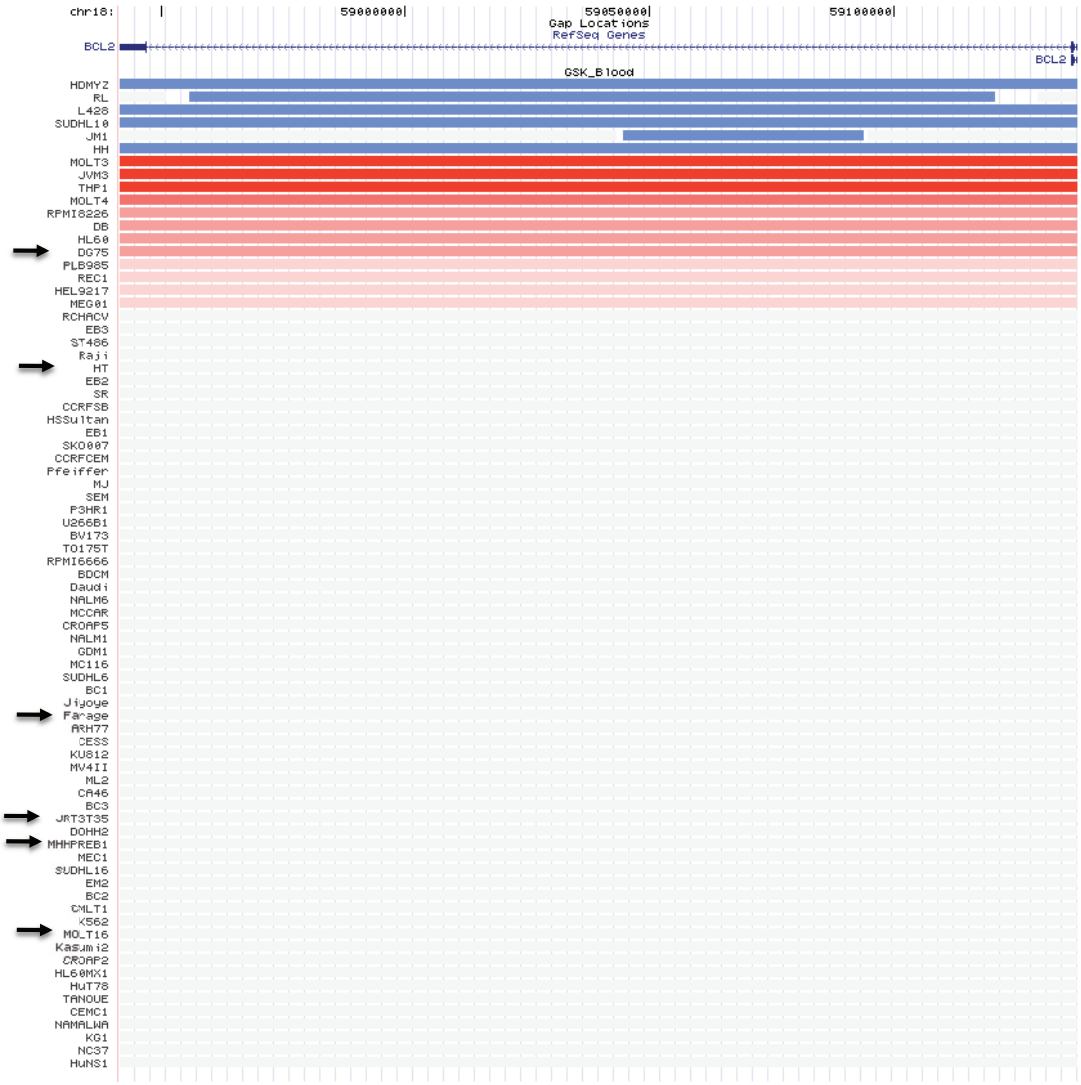
chr18:
59000000
59050000
59100000
Gap Locations
RefSeq Genes
BCL2
BCL2
GSK_Blood
HDMYZ
RL
L428
SUDHL10
JM1
HH
MOLT3
JVM3
THP1
MOLT4
RPMI8226
DB
HL60
DG75
PLB985
REC1
HEL9217
MEG01
RCHACV
EB3
ST486
Raji
HT
EB2
SR
CCRFSB
HSSultan
EB1
SKO007
CCRFCEM
Pfeiffer
MJ
SEM
P3HR1
U266B1
BV173
TO175T
RPMI6666
BDCM
Daudi
NALM6
MCCAR
CROAP5
NALM1
GDM1
MC116
SUDHL6
BC1
Jiyoye
Farage
ARH77
CESS
KU812
MV4II
ML2
CA46
BC3
JRT3T3
DOHH2
MHHPREB1
MEC1
SUDHL16
EM2
BC2
CMLT1
K562
MOLT16
Kasumi2
CROAP2
HL60MX1
HWT78
TANOUE
CEMC1
NAMALWA
KG1
NC37
HuNS1

Supplementary Figure 11. The *FBXO11* gene is deleted in hematopoietic cell lines more often than in other types of cell lines.

a, A High-Density, Single Nucleotide Polymorphism (HD-SNP) inferred copy number heat map of the *FBXO11* locus in 77 hematopoietic cell lines is shown. The data were gathered from the GSK cancer cell line genomic profiling database (https://cabig.nci.nih.gov/caArray_GSKdata/) analyzed via the Cancer Genome Atlas data portal (http://cancergenome.nih.gov/). The table on the right summarizes the number of *FBXO11* deletions identified in 332 cell lines.

b, An HD-SNP inferred copy number heat map of the *FBXO11* locus in 255 non-hematopoietic cell lines (obtained from the same GSK database) is shown.

c, An HD-SNP inferred copy number heat map of the *BCL6* locus in 77 hematopoietic cell lines (obtained from the same GSK database) is shown. The arrows indicate cell lines with *FBXO11* deletions.

d, An HD-SNP inferred copy number heat map of the *BCL2* locus in 77 hematopoietic cell lines (obtained from the same GSK database) is shown. The arrows indicate cell lines with *FBXO11* deletions.

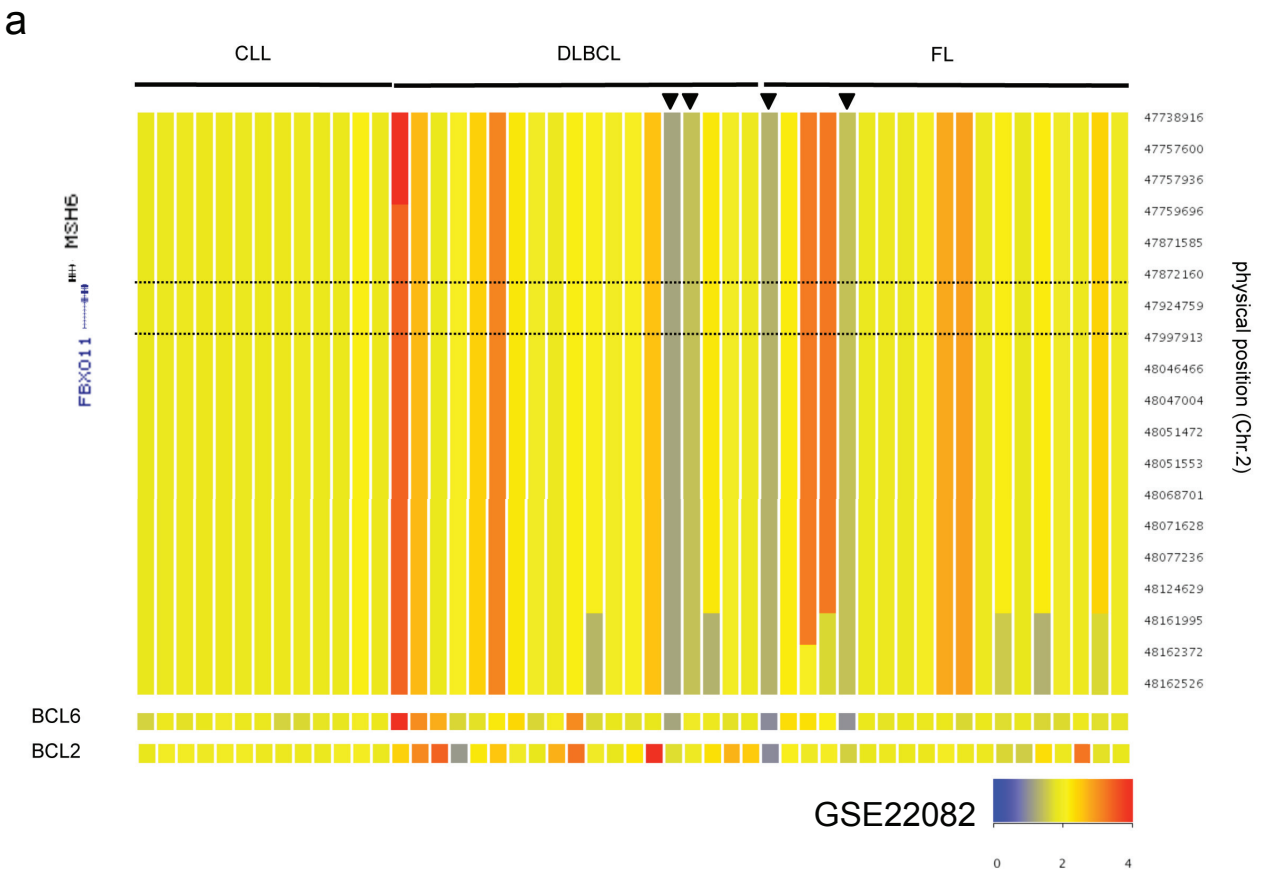

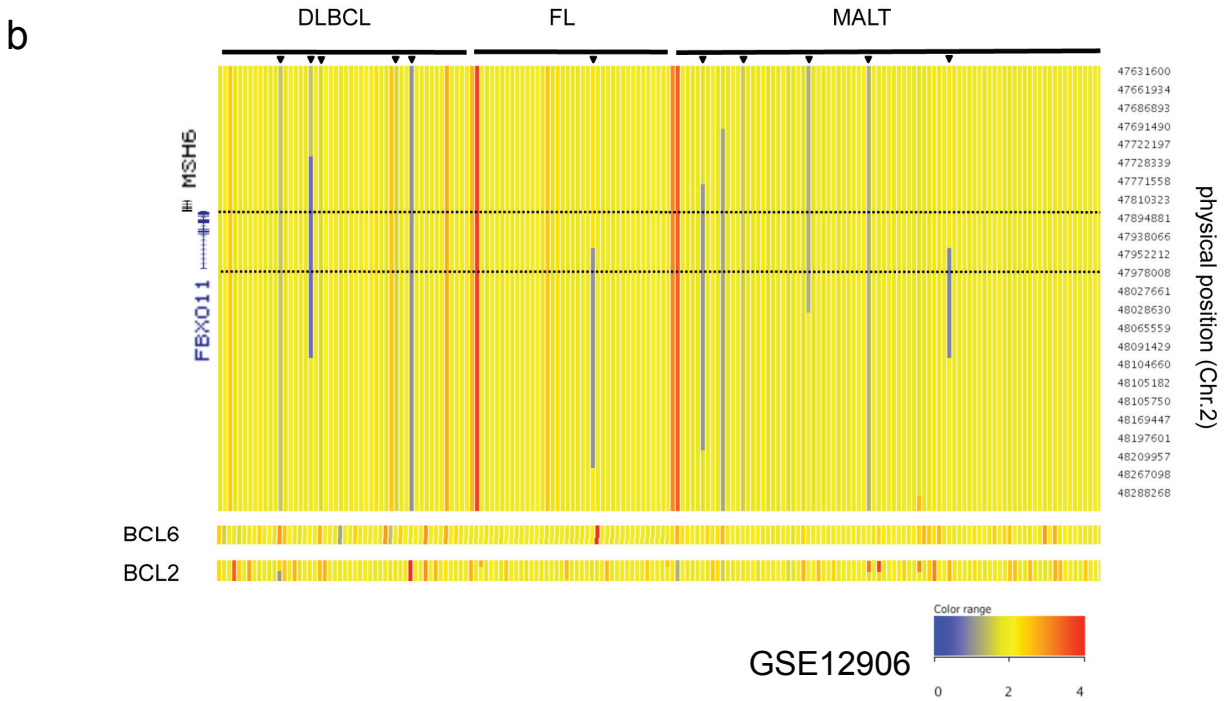

DATASETS (GEO – DATABASE)		GSE12906			GSE22082			GSE22208
	ORIGIN	DLBCL	FL	MALT	CLL	DLBCL	FL	DLBCL CELL LINES (Shipp's Lab)
SAMPLE #		50	39	84	13	19	19	27
DELETION IN FBXO11 LOCUS (#)		4	1	6	0	2	2	4
DELETION IN FBXO11 LOCUS (%)		8%	2%	7%	0	10.5%	10.5%	14.8%

Supplementary Figure 12. The *FBXO11* gene is deleted in primary DLBCLs.

a, Affymetrix 250K Sty HD-SNP array copy number data of the *FBXO11* locus in 13 Chronic Lymphocytic Leukemia (CLL) samples, 19 DLBCLs, and 19 Follicular Lymphomas (FL) is shown. The status of the *BCL6* and *BCL2* loci is also shown. Data are accessible at the NCBI-GEO database[7], accession # GSE22082 ([9]).

b, Affymetrix 250K Nsp HD-SNP array copy number data of the *FBXO11* locus in 50 DLBCLs, 39 FLs, and 84 Mucosa-Associated Lymphoid Tissue lymphomas (MALTs) is shown. The status of the *BCL6* and *BCL2* loci is also shown. The data are accessible at the NCBI-GEO database[7], accession # GSE12906 (ref [10]).

The table at the bottom summarizes the number of *FBXO11* deletions identified by the three studies reported in Supplementary Fig. 10 and 12.

a

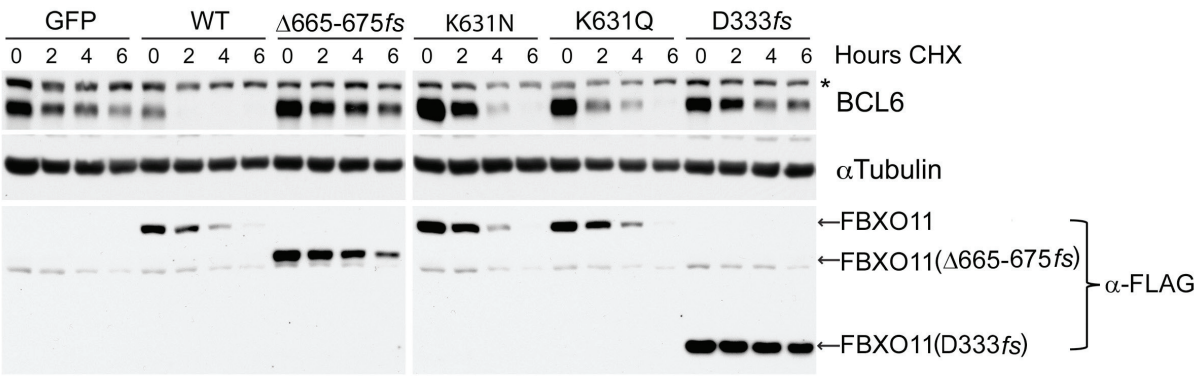
GFP
WT
Δ665-675fs
K631N
K631Q
D333fs
0 2 4 6 0 2 4 6 0 2 4 6 0 2 4 6 0 2 4 6 0 2 4 6
Hours CHX
*
BCL6
αTubulin
←FBXO11
←FBXO11(Δ665-675fs)
←FBXO11(D333fs)
α-FLAG

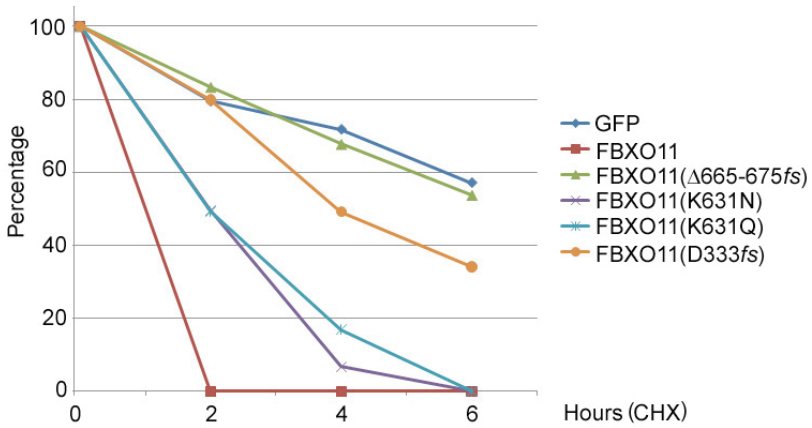
Percentage
100
80
60
40
20
0
0
2
4
6
Hours (CHX)
GFP
FBXO11
FBXO11(Δ665-675fs)
FBXO11(K631N)
FBXO11(K631Q)
FBXO11(D333fs)

b

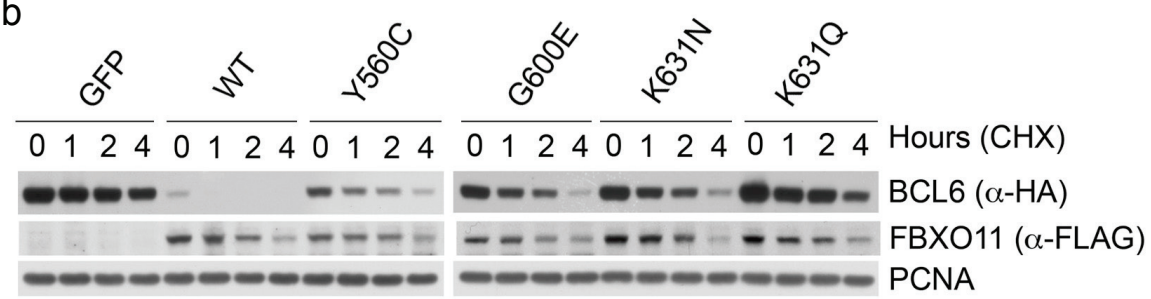
GFP
WT
Y560C
G600E
K631N
K631Q
0 1 2 4 0 1 2 4 0 1 2 4 0 1 2 4 0 1 2 4 0 1 2 4
Hours (CHX)
BCL6 (α-HA)
FBXO11 (α-FLAG)
PCNA

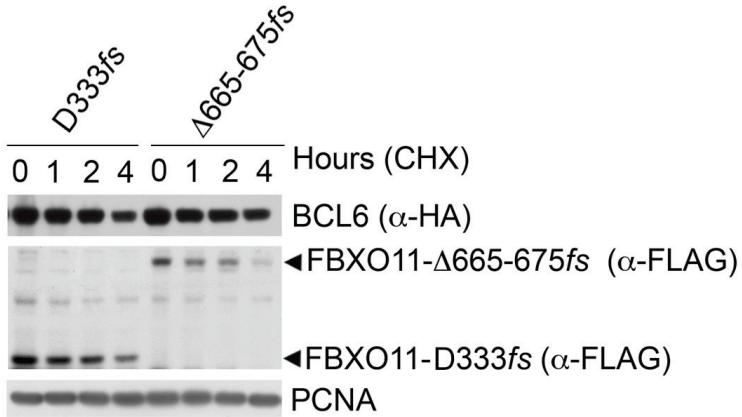
D333fs
Δ665-675fs
0 1 2 4 0 1 2 4
Hours (CHX)
BCL6 (α-HA)
◀FBXO11-Δ665-675fs (α-FLAG)
◀FBXO11-D333fs (α-FLAG)
PCNA

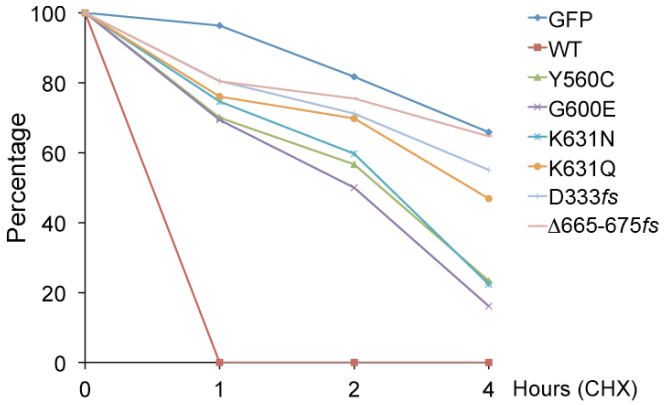
Percentage
100
80
60
40
20
0
0
1
2
4
Hours (CHX)
GFP
WT
Y560C
G600E
K631N
K631Q
D333fs
Δ665-675fs

Supplementary Figure 13. FBXO11 tumor-derived mutants have an impaired ability to induce BCL6 degradation.

a, HEK-293T cells were transfected with BCL6 in combination with GFP, FLAG-tagged wild type (WT) FBXO11, or the indicated FLAG-tagged FBXO11 tumor-derived mutants. Twenty-four hours post-transfection, cells were treated with cycloheximide (CHX), and samples were harvested at the indicated time points for immunoblotting. The asterisks denote non-specific bands that are used for normalization. The graph shows the quantification of BCL6 over the time course. The intensity of the bands from the experiment shown in the upper blot was measured using Image-Pro Plus 6.0 software (Media Cybernetics). The ratio between the relative levels of BCL6 and α–Tubulin in each time 0 was set as 100%.

b, HEK-293T cells were transfected with BCL6 in combination with GFP, FLAG-tagged wild type (WT) FBXO11, or the indicated FLAG-tagged FBXO11 tumor-derived mutants. Twenty-four hours post-transfection, cells were treated with cycloheximide (CHX), and samples were harvested at the indicated time points for immunoblotting. The graph shows the quantification of BCL6 over the time course. The intensity of the bands from the experiment shown was measured using Image-Pro Plus 6.0 software (Media Cybernetics). The ratio between the relative levels of BCL6 and PCNA in each time 0 was set as 100%.

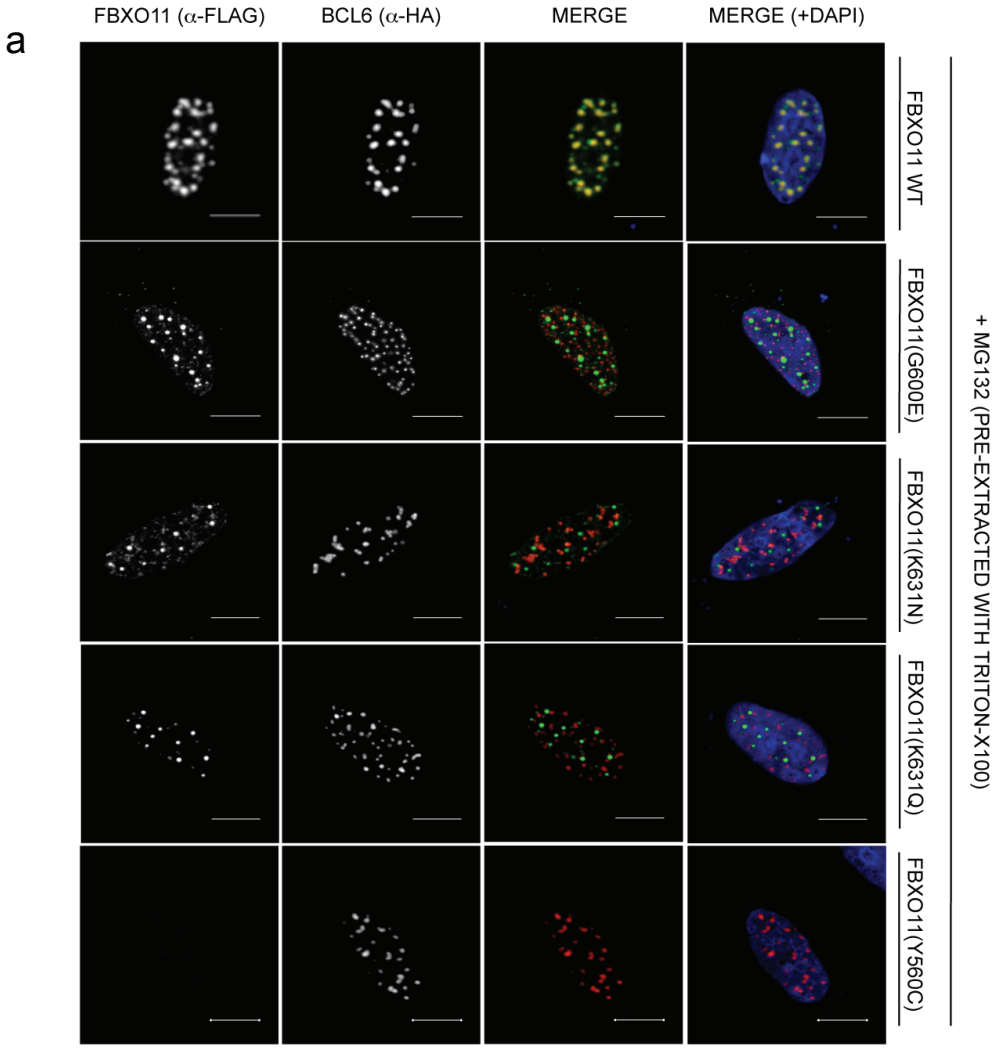
a
FBXO11 (α-FLAG)
BCL6 (α-HA)
MERGE
MERGE (+DAPI)
FBXO11 WT
FBXO11(G600E)
FBXO11(K631N)
FBXO11(K631Q)
FBXO11(Y560C)
+ MG132 (PRE-EXTRACTED WITH TRITON-X100)

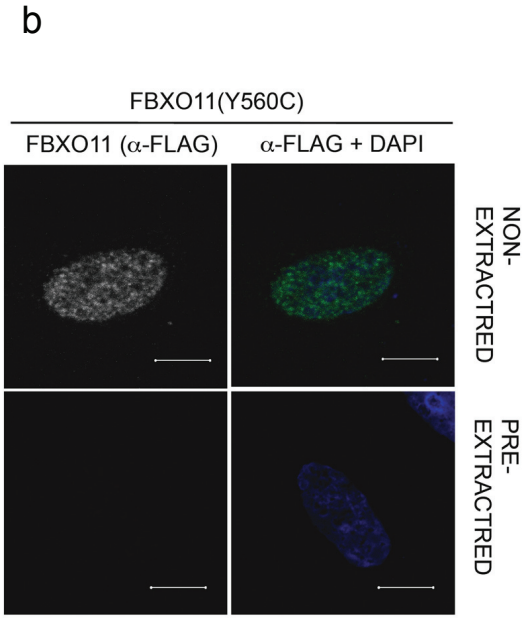
b
FBXO11(Y560C)
FBXO11 (α-FLAG)
α-FLAG + DAPI
NON-EXTRACTRED
PRE-EXTRACTRED

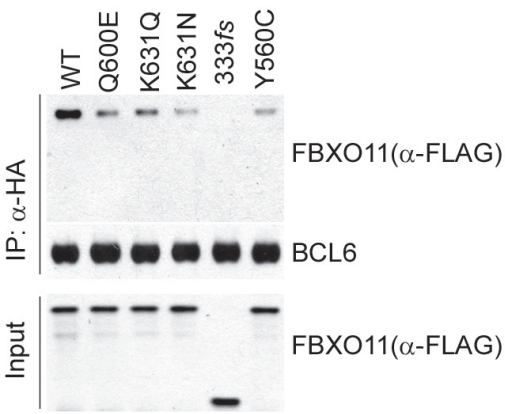
c
WT
Q600E
K631Q
K631N
333fs
Y560C
IP: α-HA
Input
FBXO11(α-FLAG)
BCL6
FBXO11(α-FLAG)

Supplementary Figure 14. Tumor-derived FBXO11 mutants do not colocalize with BCL6 and bind BCL6 less efficiently than wild type FBXO11.

a, U-2 OS cells were transfected with HA-tagged BCL6 and either FLAG-tagged wild type (WT) FBXO11 or the indicated FLAG-tagged FBXO11 tumor-derived mutant. Twenty-four hours after transfection, cells were incubated with MG132 for four hours, pre-extracted with 0.5% Triton-X100, and immunostained as indicated. In the merged image, yellow shows colocalization of FBXO11 and BCL6. FBXO11(Y560C) was not detected because the Y560C mutation makes FBXO11 Triton-soluble, as shown in *b*.

b, U-2 OS cells were transfected with FLAG-tagged FBXO11(Y560C). Twenty-four hours after transfection, cells were incubated with MG132 for four hours and immunostained as indicated. Soluble nuclear proteins in the cells shown in the bottom panels were pre-extracted with 0.5% Triton-X100 prior to immunostaining. In the merged image, yellow shows colocalization of FBXO11 and BCL6. FBXO11(Y560C) was only detected in non-extracted cells, indicating that the Y560C mutation makes FBXO11 Triton-soluble.

c, HEK-293T cells were transfected with BCL6 in combination with GFP, FLAG-tagged wild type (WT) FBXO11, or the indicated FLAG-tagged FBXO11 tumor-derived mutants. Twenty-four hours after transfection, cells were harvested and lysed. Whole cell extracts (WCE) were subjected to immunoprecipitation (IP) with anti-HA resin (α-HA) and immunoblotting as indicated.

Case #	Year	Age	Gender	Location	Diagnosis	Previous lymphoma	Sample origin	clonality	BCL2 rear.	CD10	MUM1/IRF4	BCL6	TYPE
1	2008	56	M	Stomach	DLBCL		Esophagus + Liver	Clonal FR3	-	+	+	ND	GCB
2	2008	81	F	Subcutaneous	DLBCL		LN	Polyclonal FR2	+	-	+	-	ABC
3	2008	69	M	Spleen	DLBCL		Spleen	Clonal FR3	-	-	+	+	ABC
4	2008	68	F	Inguinal LN	DLBCL		LN	Clonal FR3	+	-	+	-	ABC
5	2008	67	M	Spleen	DLBCL		Spleen	Clonal FR2	-	-	+	-	ABC
6	2008	75	M	Axillary LN	DLBCL		LN	ND	ND	-	+	-	ABC
7	2008	74	M	Axillary LN	DLBCL		LN	Clonal FR2	-	-	+	+	ABC
8	2008	50	M	Cervical LN	DLBCL		LN	Clonal FR2	-	-	+	+	ABC
9	2008	52	M	Ileal LN	DLBCL		LN	Clonal FR3	+	+	-	+	GCB
10	2008	93	F	Cervical LN	DLBCL		LN	Clonal FR2	-	+	-	+	GCB
11	2008	53	M	Axillary LN	DLBCL		LN	Clonal FR3	-	-	+	-	ABC
12	2008	29	M	Axillary LN	DLBCL		LN	Polyclonal FR2	-	-	-	+	GCB
13	2008	79	M	Inguinal LN	DLBCL	GL (1999)	LN	Clonal FR2	-	-	+	-	ABC
14	2008	76	F	Mesenteric LN	DLBCL		OMENTUM	Clonal FR3	-	+	+	+	GCB
15	2008	83	F	Spleen	DLBCL		LN	Clonal FR2	ND	-	+	+	ABC
16	2008	54	M	Axillary LN	DLBCL	CL (2007)	LN	Polyclonal FR2	-	-	-	+	GCB
17	2008	22	M	large bowel	DLBCL		Small intestine	Clonal FR3	-	+	-	+	GCB
18	2008	73	F	Cervical LN	DLBCL		LN	Polyclonal FR2	-	-	+	-	ABC
19	2008	58	M	Abdominal mass	DLBCL		Abnominal Mass	Clonal FR2	-	+	-	+	GCB
20	2008	62	M	Axillary LN	DLBCL		LN	Clonal FR2	+	-	-	+	GCB
21	2008	55	M	Inguinal mass	DLBCL		Inguinal mass	Clonal FR2	-	-	-	+	GCB
22	2008	80	M	Tibial mass	DLBCL		Pretibial Mass	Clonal FR2	-	-	+	+	ABC
23	2008	53	M	Cervical LN	DLBCL		LN	Clonal FR3	-	-	+	+	ABC
24	2008	72	M	Axillary LN	DLBCL		LN	Clonal FR2	-	+	-	+	GCB
25	2008	71	F	Axillary LN	DLBCL		LN	Clonal FR2	ND	-	ND	-	ABC
26	2008	69	F	Spleen	DLBCL		Spleen	Clonal FR2	-	-	ND	ND	ND
27	2008	72	M	Cervical LN	DLBCL		Lateral Cervical Node	Clonal FR2	-	-	ND	ND	ND
28	2008	64	F	Mesenteric LN	DLBCL		LN	Clonal FR2	-	-	+	ND	ABC
29	2008	50	F	Pharyngeal mass	DLBCL	HL (2002)	Pharynx Mass	Clonal FR2	ND	-	+	+	ABC
30	2008	52	F	Supraclavicular LN	DLBCL		LN	Clonal FR2	+	+	-	+	GCB
31	2009	45	M	Axillary LN	DLBCL		LN	Clonal FR2	-	+	-	+	GCB
32	2009	80	M	Inguinal LN	DLBCL		LN	Clonal FR2	-	-	+	ND	ABC
33	2009	75	M	Cervical LN	DLBCL		LN	Clonal FR3	+	+	+	+	GCB
34	2009	72	F	aortic mass	DLBCL			Polyclonal FR2	-	-	+	-	ABC
35	2009	71	F	Supraclavicular LN	DLBCL		LN	Clonal FR2	+	+	ND	+	GCB
36	2009	69	F	Supraclavicular LN	DLBCL		LN	Clonal FR2	-	-	+	-	ABC
37	2009	75	M	Spleen	DLBCL		Spleen	Clonal FR2	+	+	-	+	GCB
38	2009	55	F	Abdominal mass	DLBCL		Abnominal Mass	Clonal FR3	-	-	+	-	ABC
39	2009	76	F	Inguinal LN	DLBCL		LN	Clonal FR2	-	+	+	+	GCB
40	2009	25	F	Small intestine	DLBCL		jejunum	Clonal FR2	ND	+	ND	ND	GCB
41	2009	72	M	Lung mass	DLBCL	MZL (2001)	LN	Clonal FR2	-	-	+	-	ABC
42	2009	62	F	Small intestine	DLBCL		jejunum	Clonal FR3	-	-	+	+	ABC
43	2009	74	F	Abdominal mass	DLBCL		Peritoneal Nodes	Clonal FR2	-	+	-	ND	GCB
44	2009	56	M	Inguinal LN	DLBCL		LN	Clonal FR2	-	+	-	+	GCB
45	2009	60	M	Vertebral mass	DLBCL		Incisional Biopsy	Clonal FR2	-	+	-	+	GCB
46	2009	89	F	Inguinal LN	DLBCL		LN	Clonal FR2	-	+	+	+	GCB
47	2009	64	F	Axillary LN	DLBCL		LN	Clonal FR3	-	-	-	-	ND
48	2009	70	M	Inguinal LN	DLBCL		LN	Clonal FR2	-	+	+	+	GCB
49	2009	72	M	Unspecified LN	DLBCL		LN	Clonal FR3	-	-	+	-	ABC
50	2009	72	F	Inguinal LN	DLBCL		LN	Clonal FR3	-	-	+	+	ABC
51	2009	70	F	Cervical LN	DLBCL		LN	Clonal FR2	-	+	+	+	GCB
52	2009	85	M	Abdominal mass	DLBCL		LN	Clonal FR3	-	-	+	-	ABC
53	2010	70	M	Supraclavicular LN	DLBCL		LN	Polyclonal FR2	-	-	+	+	ABC
54	2010	54	M	Supraclavicular LN	DLBCL		LN	Clonal FR3	-	-	+	+	ABC
55	2010	62	F	Inguinal LN	DLBCL		LN	Clonal FR2	-	+	+	ND	GCB
56	2010	71	M	Cervical LN	DLBCL		LN	Clonal FR2	-	-	+	+	ABC
57	2010	81	M	Supraclavicular LN	DLBCL		LN	Clonal FR3	-	-	+	+	ABC
58	2010	53	F	Cervical LN	DLBCL	FL (2000)	LN	ND	+	-	-	+	GCB
59	2010	62	F	Cervical LN	DLBCL		LN	Clonal FR2	ND	-	+	+	ABC
60	2010	83	M	Axillary LN	DLBCL		LN	Clonal FR2	-	-	-	-	ND
61	2010	61	M	Inguinal LN	DLBCL		LN	Clonal FR2	-	-	ND	+	ND
62	2010	69	M	Cervical LN	DLBCL		LN	Clonal FR1 FR2 FR3	-	-	+	+	ABC
63	2010	57	M	Supraclavicular LN	DLBCL		LN	Clonal FR1 FR2 FR3	+	-	+	+	ABC
64	2010	71	F	Stomach	DLBCL		Stomach	Clonal FR1 FR2 FR3	+	-	+	+	ABC
65	2010	63	F	Skin	DLBCL		LN	Clonal FR2	ND	-	+	ND	ABC
66	2010	63	M	Inguinal LN	DLBCL		LN	Clonal FR1 FR2 FR3	-	+	ND	+	GCB
67	2005	70	M	Lung mass	DLBCL		Lung biopsy	Clonal FR2	-	+	ND	ND	GCB
68	2006	66	F	Axillary LN	DLBCL		Axillary Mass	Clonal FR2	+	-	+	ND	ABC
69	2005	50	M	Spleen	DLBCL		Spleen	Clonal FR3	+	-	ND	-	ABC
70	2006	79	F	Cervical LN	DLBCL		LN	Clonal FR3	-	-	+	+	ABC
71	2006	83	F	Axillary LN	DLBCL		LN	Clonal FR3	-	-	ND	ND	ND
72	2006	66	M	Cervical LN	DLBCL		LN	Clonal FR2	-	-	+	-	ABC
73	2005	44	F	Crural mass	DLBCL		LN	Clonal FR2	ND	+	+	+	GCB
74	2006	50	M	Cervical LN	DLBCL	CLL (2004)	LN	Clonal FR3	-	-	ND	ND	ND
75	2006	28	M	Inguinal LN	DLBCL		LN	Clonal FR3	-	+	ND	+	GCB
76	2006	75	F	Axillary LN	DLBCL		LN	Clonal FR2	-	-	ND	ND	ND
77	2006	76	F	Mediastinal LN	DLBCL	IL (2001)	LN	Clonal FR2	ND	-	ND	ND	ND
78	2006	49	F	Cervical LN	DLBCL		Lateral Cervical Node	Clonal FR3	-	-	ND	ND	ND
79	2006	80	M	Supraclavicular LN	DLBCL		LN	Clonal FR3	-	-	+	-	ABC
80	2006	80	F	Inguinal LN	DLBCL		LN	Clonal FR2	-	-	+	+	ABC
81	2006	68	F	Supraclavicular LN	DLBCL		LN	Polyclonal FR2	-	-	+	+	ABC
82	2005	64	F	Cervical LN	DLBCL		Abdominal Mass	Clonal FR2	+	-	+	+	ABC
83	2006	67	M	Inguinal LN	DLBCL		LN	Clonal FR2	-	-	ND	ND	ND
84	2006	71	F	Supraclavear LN	DLBCL		LN	Clonal FR2	-	+	ND	+	GCB
85	2006	75	F	Axillary LN	DLBCL	DLBCL (2000)	LN	Clonal FR2	-	-	+	-	ABC
86	2005	61	M	Abdominal mass	DLBCL		Retroperitoneal Mass	Clonal FR2	+	+	ND	+	GCB
87	2006	53	M	Spleen	DLBCL		Spleen	Clonal FR3	ND	-	ND	ND	ND
88	2005	52	M	Inguinal LN	DLBCL		LN	Polyclonal FR2	-	-	+	-	ABC
89	2006	77	F	Spleen	DLBCL		Spleen	Clonal FR2	-	-	+	+	ABC
90	2006	44	F	Axillary LN	DLBCL		LN	ND	ND	+	+	+	GCB
91	2006	49	M	Abdominal mass	DLBCL		LN	Clonal FR2	ND	-	+	+	ABC
92	2006	48	F	Axillary LN	DLBCL		LN	Clonal FR2	-	-	+	+	ABC
93	2006	69	F	Supraclavear LN	DLBCL		LN	Clonal FR3	ND	-	+	+	ABC
94	2010	50	F	Cervical LN	DLBCL w/FL c		Bulk Mass	Clonal FR2	-	+	ND	+	GCB
95	2010	37	F	Axillary LN	DLBCL w/FL c		LN	Polyclonal FR2	+	+	-	+	GCB
96	2010	50	F	Cervical LN	DLBCL	MZL (2010)	LN	Clonal FR3	ND	-	+	-	ABC
97	2010	38	F	Cervical LN	DLBCL w/MZL c		LN	Clonal FR3	ND	-	+	-	ABC
98	2010	72	F	Thyroid gland	DLBCL		Thyroid Nodule	Clonal FR3	-	+	+	+	GCB
99	2010	60	M	Skin	DLBCL		LN	Clonal FR3	+	+	ND	+	GCB
100	2010	76	M	inguinal LN	DLBCL		LN	Clonal FR3	-	-	+	+	ABC

Supplementary Table 1

Genomic DNA from 100 DLBCL patients was obtained from the archives of the Department of Biomedical Sciences and Human Oncology of the University of Torino and San Giovanni Battista Hospital (Turin, Italy) after approval by the Institutional Review Board. DLBCL lymphoma patients are listed according to clinical features (sex, age, and site of origin), clonality of the Immunoglobulin heavy chain gene (*IgH*), and *BCL2-IgH* gene rearrangements by PCR using a PCR technique that amplifies the major breakpoint region site of the *BCL2* gene. Of the 100 samples analyzed, 87 were primary DLBCLs and 13 were relapses or transformations of a previous lymphoma. DLBCLs were stratified into Germinal Center (GCB)- or Activated B-cell (ABC)-type by immunohistochemistry with antibodies to CD10, BCL6, and MUM1/IRF4, according to the classification proposed by Hans *et al*.[11]. Abbreviations: GL (Gastric Lymphoma), CL (Cutaneous Lymphoma), HL (Hodgkin Lymphoma), FL (Follicular lymphoma), MZL (Marginal Zone Lymphoma), CLL (Chronic Lymphoblastic Lymphoma), IL (Immunoblastic Lymphoma), LN (Lymph Node), DLBCL w/FL c (DLBCL with FL component), DLBCL w/MZL c (DLBCL with MZL component), ND (Not Determined).

cell line/tumor sample	changes in the BCL6 locus
OCI-LY1	gain in 3q21-3q29 and one mutation in BSE1*
FARAGE	no translocations and no mutations in BSE1
HT	no translocations and no mutations in BSE1
MHHPREB1	no translocations and no mutations in BSE1
CASE#15	no translocations and no mutations in BSE1
CASE#21	no translocations and no mutations in BSE1
CASE#30	no translocations or mutations in BSE1
CASE#95	no translocations and no mutations in BSE1

Supplementary Table 2

Cell lines and DLBCL samples with *FBXO11* dysregulation were analyzed for *BCL6* translocations (using FISH) and mutations in the BCL6 promoter [BCL6 binding site in exon 1 (BSE1)], which makes BCL6 insensitive to its negative autoregulation[12,13]. The only cases in which BCL6 and *FBXO11* dysregulation coexist is in OCI-LY1 cells, in which we found one mutation in the BSE1 motif (TTC to TCC in position +256-258 from the BCL6 promoter), as previously reported for this cell line[12,13]. Moreover, OCI-LY1 cells have an extra copy of BCL6. Although the co-occurrence of *BCL6* and *FBXO11* alterations in the same cell line may seem counterintuitive, cooperation between two independent genetic events is consistent with previous observations. For example, in Burkitt's and other lymphomas, high levels of c-Myc are achieved via both increased transcription (due to translocations of the *c-myc* gene to the immunoglobulin loci) and escape from ubiquitin-mediated degradation (through mutation of the c-Myc phosphodegron)[14,15]. Similarly, mutations in *Huwe1*, encoding an ubiquitin ligase targeting N-Myc, coexist with *N-myc* gene amplification in human glioblasomas[16]. Because oncoproteins often display short half-lives, their accumulation in tumor cells may require both increased synthesis and stabilization by a secondary event (*i.e.* mutation of the degron or an independent loss of the gene encoding their ubiquitin ligase).

PRIMERS FOR FBXO11 GENOMIC DNA AMPLIFICATION AND SEQUENCING

FBXO11-Ex1-2F	CTCCCTCCCGAATTTGAAG	FBXO11-Ex1-2R	AAAGTCAGAGGGAGAGGTCAGG
FBXO11-Ex3F	TGTGTTACCCATGAAACCCAC	FBXO11-Ex3R	CCGACTTTCCTACCATGTTTAGC
FBXO11-Ex4F	TCTAGCCTGGATGACAGTGAGAC	FBXO11-Ex4R	CGCCCAGCCTAAACTTATTTC
FBXO11-Ex5-6F	GAAACCCTGTTCTTTGTTTCTGG	FBXO11-Ex5-6R	TCTTCATTCCTACTTTACCAGCAG
FBXO11-Ex7-8F	AGCAAAGGCTGATGATGAAA	FBXO11-Ex7-8R	GGACATGCTCCTTGACCACT
FBXO11-Ex9-10F	ACACCACAATGCACACCACT	FBXO11-Ex9-10R	GAACGCTATCACCTCTACATGG
FBXO11-Ex11F	GCCCAGCCTTAAATGTTTCTAATAC	FBXO11-Ex11R	CAATAGCTATGGCTCATTCAGATG
FBXO11-Ex12F	TGAAGAAATTGAGGCCTTAGAAGT	FBXO11-Ex12R	TCAGTGCTTCCACTTGGGTAG
FBXO11-Ex13F	GCCTGCAGCTCTCTGCATC	FBXO11-Ex13R	TTAAGATACTGGCAGGGAGAAGAAG
FBXO11-Ex14-15F	TGCCATTACCTCCTTACTCGG	FBXO11-Ex14-15R	CCAGTGGCTTCTGTCCTCAC
FBXO11-Ex16F	TTCTCAGGGCATCTTGGACTC	FBXO11-Ex16R	GTGATCCACCCATCTCGG
FBXO11-Ex17F	CCACTGCACACTCCAGCC	FBXO11-Ex17R	GGCACTAATCTCCTAAACCAGTTC
FBXO11-Ex18F	TGGAGATGGCAGATTATTGGTC	FBXO11-Ex18R	CATTCAGCCACTTCAGCACAC
FBXO11-Ex19F	ACTGTTGGTGGTTGAAATAGGTATC	FBXO11-Ex19R	TCCAACCATTTAGAACCAAAGC
FBXO11-Ex20F	GCTTTGGTTCTAAATGGTTGGAG	FBXO11-Ex20R	ACCACGCCTACCCACAGTTAC
FBXO11-Ex21-22F	GGTCCTCTTAAAGCCAAAGGTC	FBXO11-Ex21-22R	ACCCAGCTTTGAGATCCTGAG
FBXO11-Ex3-SeqF	CATTAGATAAAATGAAAACTG		
FBXO11-Ex4-SeqF	TCTTACTCAAGTTTTTGAGGC		
FBXO11-Ex9-10-SeqF	GACTATATATAACAGATCATG		
FBXO11-Ex9-10-SeqR	CATTATCCTCATATATTCCC		
FBXO11-Ex14-SeqR	AAAGCTTTTTCAAGGGACAAG		
FBXO11-Ex17-SeqF	AAATATACCTTCTAGATAACC		

PRIMERS FOR GENE COPY NUMBER ANALYSIS

		FWD	REV
FBXO11_probe #1	CHR_2(26965666-26965733)	CTCCATGACCACCACTCCTT	ATGACACAGCCCTCATCTCC
FBXO11_probe #2	CHR_2(26864659-26864712)	ACTTGGCCAATTTCAACCAG	TCAGACCCCCAATTTCAGAG
CHR5_probe #1	CHR_5 (217588-217670)	CGGATCGTTAATTTGCAGGT	GTCTCCTCCCACCACACACT
CHR5_probe #2	CHR_5(244549-244638)	GCAACAGAAGAAGCCCTTTG	ACGAGCTCCACACTGACCTT
CHR6_probe #2	CHR_6(33230146-33230235)	ACTGTTGGGAGGGAACCTCT	TCAAACAAGTCAACCCCACA
CHR12_probe #1	CHR_12(6585217-6585317)	GCTTGCCCTGTCCAGTTAAT	TAGCTCAGCTGCACCCTTTA
CHR12_probe #2	CHR_12(6587237-6587298)	AGGGCCCTGACAACTCTTTT	CCCTGTTGCTGTAGCCAAAT

PRIMERS FOR QPCR ANALYSIS OF mRNA

	FWD	REV
hFBXO11	GATGGACGAGGCCTTATTGA	TGTTATGCCGAACAATTGGA
hIRF4	CACTTGTGTGTGCGTGTCAG	TGACTGGAGAGCAATGAACG
hRPS13	CAGTCGGCTTTACCCTATCG	CCCTTCTTGGCCAGTTTGTA
hGAPDH	TGCACCACCAACTGCTTAGC	GGCATGGACTGTGGTCATGAG
hSDHA	TACAAGGTGCGGATTGATGA	GGTGTGCTTCCTCCAGTGCT

Targeting Sequences of siRNA oligos

FBXO11 siRNAs #1	GUAAAUUGUAGCCCUAUUA
FBXO11 siRNAs #2	AAUAGUGACCCAACAAUAA
FBXO11 siRNAs #3	GAAAGUUGCAAUAUACACA
FBXO11 siRNAs #4	GCAAUGCAUUAGCAGGAAU
LacZ siRNA	CGUACGCGGAAUACUUCGA
Non-targeting siRNA (NTS)	UGGUUUACAUGUCGACUAA

Targeting Sequences of shRNAs

FBXO11 shRNAs #1	GAGTTTACATCTTTGGTGA
FBXO11 shRNAs #2	CAATTGTTCGGCATAACAA
FBXO11 shRNAs #3	TGGATTAAGACAGATAGTA
FBXO11 shRNAs #4	AGGCTGTTAGTAGAGGCCA
FBXO11 shRNAs #5	AGATAGTAATCCTACACTA

Supplementary Table 3

Primers, siRNAs and shRNAs sequences used in this study.

Supplementary References

1 Benmaamar, R. & Pagano, M. Involvement of the SCF complex in the control of Cdh1 degradation in S-phase. *Cell Cycle* 4, 1230-1232, (2005).

2 Piva, R. *et al.* In vivo interference with skp1 function leads to genetic instability and neoplastic transformation. *Mol Cell Biol* 22, 8375-8387, (2002).

3 Yen, H. C. & Elledge, S. J. Identification of SCF ubiquitin ligase substrates by global protein stability profiling. *Science* 322, 923-929, (2008).

4 Kageshita, T. *et al.* Increased expression of germinal center-associated nuclear protein (GANP) is associated with malignant transformation of melanocytes. *J Dermatol Sci* 42, 55-63, (2006).

5 Alonso, S. R. *et al.* Progression in cutaneous malignant melanoma is associated with distinct expression profiles: a tissue microarray-based study. *Am J Pathol* 164, 193-203, (2004).

6 Niu, H., Ye, B. H. & Dalla-Favera, R. Antigen receptor signaling induces MAP kinase-mediated phosphorylation and degradation of the BCL-6 transcription factor. *Genes Dev* 12, 1953-1961, (1998).

7 Edgar, R., Domrachev, M. & Lash, A. E. Gene Expression Omnibus: NCBI gene expression and hybridization array data repository. *Nucleic Acids Res* 30, 207-210, (2002).

8 Green, M. R. *et al.* Integrative analysis reveals selective 9p24.1 amplification, increased PD-1 ligand expression, and further induction via JAK2 in nodular sclerosing Hodgkin lymphoma and primary mediastinal large B-cell lymphoma. *Blood* 116, 3268-3277, (2010).

9 Green & Griffiths. A genomic profiling of human lymphomas. *Unpublished*.

10 Kato, M. *et al.* Frequent inactivation of A20 in B-cell lymphomas. *Nature* 459, 712-716, (2009).

11 Hans, C. P. *et al.* Confirmation of the molecular classification of diffuse large B-cell lymphoma by immunohistochemistry using a tissue microarray. *Blood* 103, 275-282, (2004).

12 Wang, X., Li, Z., Naganuma, A. & Ye, B. H. Negative autoregulation of BCL-6 is bypassed by genetic alterations in diffuse large B cell lymphomas. *Proceedings of the National Academy of Sciences of the United States of America* 99, 15018-15023, (2002).

13 Pasqualucci, L. *et al.* Mutations of the BCL6 proto-oncogene disrupt its negative autoregulation in diffuse large B-cell lymphoma. *Blood* 101, 2914-2923, (2003).

14 Bahram, F., von der Lehr, N., Cetinkaya, C. & Larsson, L. G. c-Myc hot spot mutations in lymphomas result in inefficient ubiquitination and decreased proteasome-mediated turnover. *Blood* 95, 2104-2110, (2000).

15 Bhatia, K. *et al.* Point mutations in the c-Myc transactivation domain are common in Burkitt's lymphoma and mouse plasmacytomas. *Nature Genetics* 5, 56-61, (1993).

16 Zhao, X. *et al.* The N-Myc-DLL3 cascade is suppressed by the ubiquitin ligase Huwe1 to inhibit proliferation and promote neurogenesis in the developing brain. *Developmental Cell* 17, 210-221, (2009).